

EFFECTS OF SPECTRAL RESPONSE FUNCTION DIFFERENCES ON CO₂
SLICING WITH AN APPLICATION TO CLOUD CLIMATOLOGIES

by

Mark Allen Smalley

A thesis submitted in partial fulfillment of the requirements for the degree of

Master of Science

(Department of Atmospheric and Oceanic Sciences)

at the

UNIVERSITY OF WISCONSIN-MADISON

2011

Abstract

The combination of HIRS/2 and MODIS measurements provide a global cirrus cloud climatology with over 30 years of combined observations. However, the sensitivity of cloud height retrievals using CO₂ slicing to spectral differences between the different HIRS/2 and MODIS instruments has not been well characterized, providing the motivation for this study. To estimate biases in retrieved cloud heights resulting from variations in spectral response functions between these instruments, cloud heights for HIRS/2 and MODIS instruments are simulated using high spectral resolution measured radiances from AIRS and the line-by-line radiative transfer model LBLRTM. As a second study, measurement spectral response functions (SRFs) are held constant while the forward model response functions are incrementally shifted. Two days of simulated cloud top heights (CTHs) for these narrow band sensors are analyzed to quantify inter-satellite biases. Because the HIRS/2 and MODIS heights are simulated using the same AIRS measurements, one-to-one comparisons exclude all sources of error except the differing spectral response functions.

It is demonstrated that the differences in narrow band CO₂ channel SRFs from pre-launch MODIS-Aqua and HIRS/2 instruments produce small, but statistically significant differences in the heights generated with CO₂ slicing. MODIS-Aqua channel combination 36/35 and analogous HIRS channels 4/5 show the smallest spread in mean cloud heights. These results suggest that biases due to SRF differences between sensors should be corrected in a long-term satellite cloud height climatology using CO₂ slicing.

To observe the sensitivity of CO₂ slicing to errors in the knowledge of the measurement SRFs, incremental linear shifts are applied to the forward model response functions while the measurement response functions are held constant. This research shows

that MODIS-Aqua channel combination 36/35 is the least sensitive to errors in forward model response functions. This is the preferential band combination in the MODIS collection 5 cloud retrieval algorithm.

Well-calibrated hyperspectral radiance measurements are useful in the construction of a long-term cloud height record because they have the flexibility to be convolved to any set of response functions. These instruments are relatively new; so long-term datasets consisting solely of hyperspectral measurements will not be available for many years. The small, but systematic differences between simulated instruments suggest that hyperspectral observations convolved to the HIRS/2 SRFs will provide the optimal continuation of the HIRS/2 climatology, as errors resulting from differences in satellite SRFs are eliminated.

Acknowledgements

I would like to first extend my gratitude to my research advisor Bob Holz for his guidance during my M.S. research at this university. His patience and thoughtful suggestions paved the way for this research to come to fruition.

I would also like to thank Steve Ackerman for creating an excellent work environment for his CIMSS graduate students. I did not expect the amount of research freedom and opportunities granted to me as a first-year graduate student in a new field.

The courses offered to graduate students by this department granted me the knowledge and skills necessary to complete an advanced degree in the atmospheric sciences. My many thanks go to the instructors of these courses, and I hope their quality instruction continues so other students may receive the same advantages I received.

I would not have been able to complete this research without the peer support from my fellow graduate students and past officemates. Their friendship and encouragement gave me the confidence I needed to get through the rigorous first year of graduate studies and complete my degree.

Finally and most importantly, I want to extend my deepest gratitude to my parents Don and Pam and my sister Jenna. Their loving support and encouragement enabled me to concentrate on my studies while knowing that I had someone there for me at all times.

Table of Contents

1. Introduction	1
2. Previous Climatology Studies	4
2.1. ISCCP	4
2.2. UW Pathfinder	5
2.3. PATMOS and PATMOS-X	6
3. Introduction to CO ₂ slicing	7
3.1. Instrument Spectral Response Functions	8
3.2. Experiment Design	9
3.3. The CO ₂ slicing equation	10
3.4. Assumptions and sources of uncertainty	13
4. Instruments and tools	19
4.1. AIRS	19
4.2. CALIOP	20
4.3. HIRS/2	21
4.4. MODIS	22
4.5. Forward model/LBLRTM	22
4.6. Ancillary profiles	24
5. Experiment and algorithm design	25
5.1. Collocation	25
5.2. Cloud top height simulator algorithm	26
5.3. Radiance bias correction	28
5.4. Scene selection	29
6. Data Sources	31
6.1. AIRS	31
6.2. CALIOP	31
6.3. GDAS	32
6.4. AFGL	32
6.5. HIRS/2 SRF	32
6.6. MODIS SRF	33
7. Results	34
7.1. Selected scene characteristics	34
7.2. Case study of retrieved heights	35
7.3. Effects of radiance bias correction	37
7.4. Comparison to MODIS collection 6 cloud height product	39
7.5. Differences from CALIOP lidar observations	40
7.6. Differences from HIRS06	42
7.7. Significance	44
7.8. Dependence on optical depth	46
7.9. Uncertainties in pre-launch measurements of SRF	48
8. Discussion	51
8.1. Summary of experiment	51
8.2. Significance to UW Pathfinder	51
8.3. Forward model SRF shifts	52
9. Future Work	53
References	54

1. Introduction

Clouds play a critical role in the radiation budget of the earth through their reflection of solar radiation and absorption of terrestrial radiation. Cirrus clouds can be defined as having optical depths less than 3.6 and heights above 440mb (Rossow & Schiffer, 1999). At these high altitudes clouds are composed almost entirely of irregularly shaped ice crystals, as opposed to spherical water. The non-spherical shapes of cirrus ice crystals can create the visual effects of halos and sundogs, which have been observed for centuries (Petty, 2006).

Lidar measurements from satellites have estimated the global cirrus cloud frequency to be 16.7% (Sassen et al, 2008), while passive measurements have found high clouds of all optical depths in about 33% of all scenes (Wylie et al, 2005). Because of their prevalence and location in the upper troposphere, cirrus clouds often represent one of the first interactions of incoming solar radiation and the last interaction of outgoing radiation with the atmosphere. At altitudes above 440mb, the atmosphere is usually much colder than the underlying surface. Optically thin cirrus clouds have low solar reflectance but are still efficient at absorbing infrared radiation emitted by the surface and atmosphere, creating a greenhouse heating effect that is described Stephens and Webster (1981). Boltzman's law tells us that the energy lost to space by a column containing a cold cloud is much less than the energy lost under clear conditions. Because the atmospheric temperature lapse rate is non-zero in the troposphere, accurate knowledge of the local cloud heights is necessary to characterize the small and large-scale radiation budget.

Cirrus clouds can have significant effects on local radiation budgets, so models attempting to predict future climates need to accurately represent them. Efforts to capture the cirrus/climate feedbacks in global circulation models (GCM) have significant uncertainties

(Stephens, 2005). Senior and Mitchell (1993) found that with three different parameterizations for clouds, the effects of a doubling of atmospheric CO₂ on surface temperature can vary between 1.9 and 5.4°C, where the CO₂ greenhouse effect alone comprises just under 1 degree. On the current understanding of cloud/climate feedbacks in models, Stephens (2005) explains...

... the relationship between convection, cirrus anvil clouds, and SST is a recurring theme in many feedback hypotheses... yet the connections between convection and cirrus in parameterization schemes is highly uncertain, in many cases empirical, and difficult to evaluate with observations. This is one area where observations are needed to evaluate cloud parameterization processes and feedbacks derived from these processes.

At the time of this writing, remote sensing weather satellites have been orbiting our planet for more than 50 years. Knowledge gained from these satellite measurements may be used to create long-term climatologies of cloud amounts, heights, and other important radiative atmospheric qualities, allowing researchers to assess the current climatological state as well as validate different cloud schemes in column and global radiative transfer models.

Historically, clouds with very low optical depths have not been measured due to their cloud signal being below the noise threshold for the narrow band sensors that have been gathering climatological data for decades. The recent addition of active lidar and radar sensors to retrieve global cloud profiles has increased our ability to understand the distributions of these thin clouds (Sassen et al, 2008). These new active techniques are able to provide accurate descriptions of the current cloud environment with higher vertical precision, but lack the ability to retrieve distributions for scenes in the past. Currently, cloud climatologies must be made using the historical measurements of narrow band sensors from

the last half-century. The advent of line-resolving instruments like AIRS and IASI (Infrared Atmospheric Sounding Interferometer) has introduced a new age of passive remote sensing. As is the focus of this paper, these instruments may be used to simulate less spectrally resolving instruments, enabling retrieval comparisons despite differences in the temporal coverage of each instrument.

In this experiment, radiances for the HIRS/2 and MODIS narrow band instruments are simulated via spectral convolution of hyperspectral AIRS observations according to the narrow band instrument's SRFs. With a single AIRS field of view (FOV), radiances are simulated for any set of response functions. These simulated narrow band radiance measurements are then used as inputs to the CO₂ slicing equation to retrieve cloud top heights. Values for the estimated clear sky radiance are computed by convolving the line-by-line transmittance and radiance outputs from a flexible forward model using ancillary model profiles as inputs. Using this simulation method, simulated cloud heights are generated for the narrow band instruments for the same cloud scenes; for a given field of view, SRFs for each simulated instrument are the only varying inputs to the CO₂ slicing equation.

The experimental design of this study is able to isolate the differences in narrow band SRFs on retrieved cloud top heights using CO₂ slicing from other sources of uncertainty discussed earlier. Collocated lidar measurements provide all parameters for clear and cloudy scene selection and a benchmark "truth" cloud height for comparisons between simulated instruments. The retrieval of cloud heights is therefore independent of scene selection.

2. Previous Climatology Studies

To better understand the macro- and microphysical properties of clouds in the earth system, several long-term cloud climatology projects have been undertaken. Three of these attempts to characterize trends and cycles in global cloud distributions are introduced in this section.

2.1 ISCCP

Rossow and Schiffer (1999) developed the International Satellite Cloud Climatology Project (ISCCP) to create a cloud climatology between July 1983 and December 1997. The ISCCP utilized the 11 μm infrared (IR) window brightness temperature method of retrieving cloud heights and amounts. As will be explained in Chapter 3, the limitation of this method is its inability to distinguish between a low, thick, warm cloud, and high, thin, cold clouds. The ISCCP cloud detection algorithm consists of a comparison of the measured brightness temperature to the brightness temperature of nearby clear FOVs and a similar radiance comparison for a visible channel. If the contrast in IR window between these FOVs is greater than a threshold value based on scene type, the scene is considered to be cloudy. Again, clouds transmissive at infrared wavelengths cause biases in this method. Visible reflectance measurements are made for additional cloud detection, but these measurements are available only during the day, so scenes containing thin cirrus are often incorrectly classified as clear for observations on the night side of the planet (Wylie et al, 2005). The ISCCP climatology finds a global cloud cover of 67%, with high clouds comprising coverage of about 22% of the earth and cirrus clouds comprising 13%, where cirrus are defined to have pressures below 440mb and optical depths below 3.6. The ISCCP finds that when the significance is set at 1%

per decade, numbers of high clouds decrease at a rate of about 1.75% per decade in the mid-latitudes over land. When all clouds are grouped together, trends are again decreasing at rates of between 1% per decade in northern mid-latitudes over land and 4.2% per decade in the southern mid-latitudes over ocean (Wylie et al, 2005).

2.2. UW Pathfinder

The UW Pathfinder cloud climatology study uses observations from the second version of the HIRS/2 instruments aboard the polar orbiting NOAA-06 and NOAA-8 through NOAA-14 satellites to estimate global cloud amount and height trends between July 1983 and September 2001. Recognizing the weakness in the ISCCP cloud mask and height algorithm, the UW Pathfinder study used the carbon dioxide absorption method for their cloud amount and height retrievals (Wylie et al, 2005). This method (CO₂ slicing) is more sensitive to optically thin clouds than the IR window BT method and will be explained in depth at the end of this chapter. Findings from the UW Pathfinder study generally contrast with the findings of the ISCCP project. The differences in the results from these studies are mostly attributed to the method of detecting and assigning heights to thin or transmissive clouds like cirrus. To create the UW Pathfinder cloud mask, a combination of a brightness temperature contrasts between nearby FOVs and a contrast between the measured radiance and the radiance computed with a forward model as with the ISCCP study, these contrasts are compared to a threshold value to determine pixel cloudiness. This hybrid cloud mask was seen to increase cloud detection to 75% of all fields of view, an increase of about 8-9% from ISCCP. High clouds ($P_c < 440\text{mb}$) were detected in roughly one third of all observations, which is between 10% and 15% more than detected by the ISCCP study (Wylie et al, 2005).

The trends in cloud properties found using the HIRS/2 instruments also differ from ISCCP. Trends in total cloud cover over the HIRS/2 record are found to be insignificant, and trends in high cloud cover are seen to increase by 2% per decade in the mid-latitudes. UW Pathfinder trends in high cloud cover are in direct contrast to the trends from ISCCP, which found global cloudiness trends to be negative for all significant values.

2.3. PATMOS and PATMOS-X

The suite of Advanced Very High Resolution Radiometer (AVHRR) instruments provides another method of assessing trends in cloud properties over time. The Pathfinder ATMOSphere project used AVHRR radiances from NOAA07, 09, 11, and 14 to build a 20-year global cloud climatology for cloud amounts (Jacobowitz et al, 2003) using the IR window brightness temperature technique. Optically thin clouds are often incorrectly classified as clear by the IR window cloud mask algorithm employed by this study. This weakness causes the PATMOS project to detect fewer high and thin clouds than the UW Pathfinder and ISCCP studies. The global cloud amount for all clouds is found to be close to 50%, with no significant trends (Jacobowitz et al, 2003). Recently, funding for the reprocessing of the entire AVHRR record has been approved and titled PATMOS-x. One of the goals of the PATMOS-x project is to use the split window technique to gain better estimates of global cloud height and amount. This research is ongoing.

3. Introduction to CO₂ slicing

Satellite climatologies require joining data from multiple satellite sensors to create estimates in cloud amount and height trends. However, inter-instrument differences in measurement properties can introduce errors into the calculations of trends. To create reliable estimates of cloud properties from climatologies, these inter-instrument biases need to be removed. The effects of these uncertainties on retrieved cloud heights are addressed in this chapter.

There are many differences in measurement characteristics between instruments, even when the instruments used in the climatology are designed to be identical. For example, when retrieving diurnal cycles of cloud properties, it is important to correct for errors resulting from satellite orbital drift. This source of error occurred for the HIRS/2 and AVHRR instruments and was corrected by the UW Pathfinder and PATMOS studies, respectively (Wylie et al, 2005). In addition, most cloud height retrieval algorithms require an *a priori* knowledge of the local atmospheric temperature, absorbing gas, and surface temperature. Over the years of satellite meteorology, the quality of these ancillary profiles has improved as the size of model grid boxes has decreased and computing power has increased.

Another potential source of bias for cloud climatologies is decreasing FOV sizes over time, as it is now possible to launch sensors with much smaller ground footprints than in the 1970's (e.g. the HIRS/2 footprint is about 17.7km, but similar bands on MODIS have footprints of only 1km). Menzel et al. (1992) found that increasing the size of the FOV increased the retrieved fraction of global high clouds. With smaller view sizes, more cloud holes are detected and more scenes are therefore classified as clear or partly clear. For larger

observational areas, small clear portions are not excluded and are included in the area defined as cloudy.

3.1. Instrument Spectral Response Functions

The source of error targeted by this study is the variation of spectral response functions (SRF) between different narrow band instruments. Instrument SRFs can be a source of bias between instruments and for each instrument, individually. The spectral response function is a measure of the efficiency of the optical devices used in radiance measurement to incoming energy relative to other frequencies contained by that channel. This measure includes inefficiencies from any optical instrumentation that incoming light must pass before impacting the detector (e.g. filters, waveguides, mirrors, apertures, etc.) as well as the detector, itself. Measurements of the expected instrument SRF are made in a lab setting prior to launch for components, but rarely for the entire constructed machine. As an example, the SRF for the narrow band imager MODIS-Aqua is shown in Figure 1.

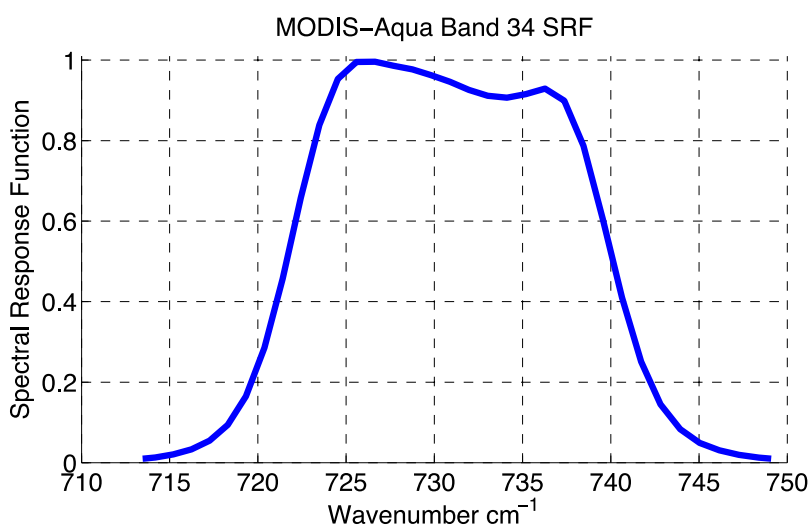


Figure 1: Sample SRF from MODIS-Aqua band 34. A band's SRF is measure of the relative amounts of radiation detected by an optical system for a flat incoming spectrum.

Figure 1 shows that if MODIS-Aqua is given a flat spectrum of radiation, light with a wavelength of 726cm^{-1} will contribute about twice as much to the radiance measurement as radiation with a wavelength of 740cm^{-1} . On-orbit calibration efforts are made to measure an instrument's SRFs because the optical qualities of a channel may change over time due to shifts during launch or as filters and detectors degrade over time. Effects of dynamic or mischaracterized response functions on retrieved cloud heights using CO_2 slicing are addressed in this experiment.

Uncertainties in retrieved cloud heights due to the differences in SRFs have not been well characterized. As mentioned above, the UW Pathfinder study leveraged the locations of HIRS/2 bands 4-7 to create a cloud climatology using CO_2 slicing. Inter-instrument biases in retrieved cloud heights were not eliminated (with the exception of the exclusion of HIRS05 and HIRS07), and could affect the estimated trends found by Wylie et al (2005). It is the goal of this research to quantify the sensitivity of retrieved heights using CO_2 slicing to differences in instrument SRFs.

3.2 Experimental Design

The introduction of high spectral resolution radiometers to the polar orbiting satellite constellations has opened up new possibilities in remote sensing research. Hyperspectral instruments like AIRS and IASI provide a means to accurately represent the radiance measured by one instrument with radiances from another instrument.

In this study, radiances for narrow band instruments HIRS/2 and MODIS are simulated via spectral convolution of measured hyperspectral AIRS observations according

to the narrow band instrument's spectral response functions. With a single AIRS field of view, radiance may be simulated for any set of response functions, meaning any narrow band instrument with bands in the CO₂ slicing region may be simulated. These simulated narrow band radiance measurements are then used as inputs to the CO₂ slicing equation to retrieve cloud top heights. The values for estimated clear sky radiance and the values on the RHS of the CO₂ slicing equation (introduced in the next section) are computed convolving the line-by-line transmittance and radiance outputs from a flexible forward model using ancillary model profiles as inputs. Using this simulation method, simulated cloud heights are generated for narrow band instruments for the exact same cloud scenes, meaning that for a given field of view, SRFs for each simulated instrument are the only varying inputs to the CO₂ slicing equation.

Through simulation of cloud heights using the same measurement FOVs, this experiment is able to isolate the effects of differences in narrow band SRFs on retrieved cloud top heights using CO₂ slicing from other sources of uncertainty, allowing for scene-by-scene comparisons and analysis. Collocated lidar measurements provide all parameters for clear and cloudy scene selection and a benchmark "truth" cloud height for comparisons between simulated instruments.

3.3 The CO₂ slicing equation

All cloud heights in this study are retrieved using the CO₂ absorption method. A full derivation of this method is given in Smith et al (1974). The utility of the CO₂ slicing method becomes apparent when one reviews the issues with using the IR window brightness

temperature method, which is a simple inversion of the Planck function (Eqn. 1) with a measured radiance $I(\nu)$ to retrieve the cloud temperature T_C .

$$\text{Equation 1} \quad I(\nu, T) = \frac{2hc^2\nu^3}{\exp\left(\frac{hc\nu}{kT}\right) - 1} \quad T_B = \frac{hc\nu}{k \ln\left(\frac{2hc^2\nu^3}{I(\nu)}\right) + 1}$$

h = Planck constant

c = speed of light in vacuum

ν = wavenumber

k = Boltzman constant

$I(\nu, T)$ = radiance at wavenumber ν and brightness temperature T

The IR window brightness temperature method is a quick and simple way to estimate the heights of clouds. Current IR brightness temperature retrievals also apply a correction for water vapor, but this does not significantly address its main weakness. The problem with this method is that it assumes that all of the radiation observed at the top of the atmosphere (TOA) originated from the cloud top, with no transmission through the cloud. For scenes with only partial cloud coverage or scenes containing transmissive clouds, this assumption is invalid. A correct description of the total radiation at the TOA can be summarized with Eqn. 2, where N is the cloud fraction, I_{cloudy} is the total radiation from the cloud-filled portion of the FOV, and I_{clear} is the total radiation from the clear portion of the FOV.

$$\text{Equation 2} \quad I_{total} = N \cdot I_{cloudy} + (1 - N) \cdot I_{clear}$$

Measurements for these scenes are contaminated with radiances from below the target cloud. Because cirrus clouds are invariably cooler than underlying clouds and surfaces, radiance contamination from below the cloud increases the brightness temperature and decreases the retrieved cloud height. So the main weakness of the IR window brightness temperature

method is that the cloud emitting temperature cannot be separated from the amount of cloud in the observation scene. In other words, a high (cold) thin cloud is indistinguishable from a low (warm) thick cloud using this method.

The CO₂ absorption method addresses this issue by dividing the TOA radiance difference imparted by the cloud for one wavelength by the same difference for another wavelength and assuming the cloud emissivity for the two frequencies are identical. This relation is known as the CO₂ slicing equation and is shown as Eqn. 3.

$$\text{Equation 3} \quad \frac{I(\nu_1) - I(\nu_1)}{I(\nu_2) - I(\nu_2)} = \frac{N\varepsilon(\nu_1) \int_0^{z_c} \tau(\nu_1, z) \frac{dB[\nu_1, T(z)]}{dz} dz}{N\varepsilon(\nu_2) \int_0^{z_c} \tau(\nu_2, z) \frac{dB[\nu_2, T(z)]}{dz} dz}$$

$I(\nu)$ = radiance for wavenumber ν

N = cloud fraction

τ = transmittance at wavenumber ν from layer z to TOA

ε = cloud emissivity

$B[\nu, T(z)]$ = blackbody emission from a layer at wavenumber ν and temperature $T(z)$

z_c = cloud height

With an assumption of an infinitesimally thin cloud, the subtraction of the cloud-cleared radiance that would exist in the absence of the cloud from the true radiance places the cloud altitude z_c as the upper limit on the integral. If the cloud emissivities, ε , for the two wavelengths ν_1 and ν_2 are identical, they fall out of the relation and the cloud height may be obtained without ambiguity from the cloud emissivity. To ensure that the division on the left hand is meaningful and not always equal to one, channels ν_1 and ν_2 are chosen such that their cloud emissivities are as close as possible, but their clear sky gas absorption emissivities are different. This is why the CO₂ slicing method works. The differing gas absorption emissivities create differences in the peaks of the clear sky weighting functions, which

produces differences in the altitudes at which each band is most sensitive to emitted energy. This occurs between the wavelengths of $13\mu\text{m}$ (770cm^{-1}) and $15\mu\text{m}$ (670cm^{-1}). The limb of the CO_2 absorption band is chosen also because CO_2 is well mixed in the atmosphere.

I_{clear} and the values in the RHS of Eqn. 3 can be computed from interpolation of retrieval products from nearby clear scenes, as was done by Wylie and Menzel (1999). Alternatively, they can also be computed directly from ancillary model profiles, as was done by Wylie et al. (2005) and is done in this experiment. To retrieve a cloud height for a given cloudy scene, a forward model computes layer-to-TOA radiances and transmittances from ancillary profiles. The left hand side (LHS) is computed, and the integrals on the right hand side (RHS) are evaluated from the surface to each potential cloud level. The retrieved cloud height is the height for which the difference between the LHS and RHS is a minimum.

3.4 Assumptions and sources of uncertainty

As with any remote sensing retrieval algorithm, there are many uncertainties associated with CO_2 slicing that can adversely affect the retrieved cloud top heights. Specific causes of retrieval uncertainty include violations of the assumptions of constant cloud emissivity between channels, geometrically thick yet optically thin clouds, and multi-layer cloud scenes. Other sources of uncertainty include scenes that are only slightly cloud-filled or contain very tenuous cirrus, errors in the radiative transfer forward model and ancillary forward model inputs, and an inadequate knowledge of the true instrument SRFs. Each of these sources of error is discussed in this section.

Identical cloud emissivity

The cloud emissivity at ν_1 has been assumed to be identical to the cloud emissivity at ν_2 . Uncertainties and biases resulting from failures of this assumption are minimized by the design of the instrument channels to be used in CO₂ slicing. These channels are placed successively on the lower limb of the 15 μ m absorption region. This spectral region displays a steady decrease in radiance due to absorption by atmospheric carbon dioxide gas as one observes radiances at increasing wavenumths. This effect is demonstrated in Figure 2, which shows a spectrum of AIRS hyperspectral measurements for a cloudless FOV with the locations of the MODIS-Aqua bands used for cloud height retrieval using CO₂ slicing.

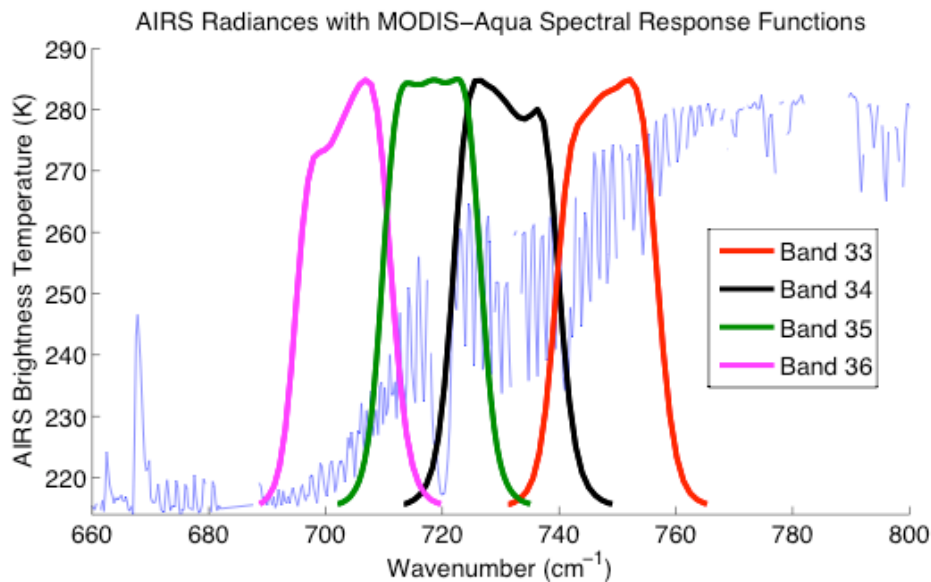


Figure 2: MODIS-Aqua bands 33-36 SRFs with AIRS brightness temperatures for a sample clear FOV in blue. Brightness temperatures decrease with decreasing wavenumber between 760 and 660 cm^{-1} as a result of absorption by atmospheric carbon dioxide.

Calculations made by Jacobowitz (1970) show changes in emissivity of ice and water clouds with wavelength are small compared to the changes in gas absorption emissivity in the limb of the 15 μ m CO₂ absorption region. The Zhang and Menzel (2002) experiment replaced the

1.0 assumed cloud emissivity ratio in the RHS of the CO₂ slicing equation with emissivity ratios computed with the radiative transfer model Streamer (Key and Schweiger, 1998). Comparisons of retrieved cloud heights with a collocated airborne lidar system (Spinhirne and Hart, 1990) show that when clouds are thin, the cloud emissivity adjustment improves retrieved cloud heights by 10-20mb. As expected, retrievals for optically thick clouds are not significantly altered by the adjustment because their high optical depths. Because these emissivity adjustments are not implemented in the MODIS collection 5 algorithm they are not included in the simulator.

Infinitesimally thin cloud layer

The integrals in the RHS of Eqn. 3 also assume that the radiation from the cloud comes from an infinitesimally thin cloud layer at altitude z_c . Using comparisons between the MODIS Airborne Simulator (MAS) and Cloud Physics Lidar (CPL), Holz et al. (2006) showed that RHS and LHS of CO₂ slicing algorithms tend to converge where the integrated lidar extinction (optical depth as viewed from the aircraft above the cloud) is 1. Since this is the region of the cloud that is most important for outgoing radiation, knowledge of the height of the optical depth equals 1 region of the cloud might be more useful for understanding radiation budgets than knowledge of the physical cloud top height. If finite cloud thicknesses were included in the RHS of the CO₂ slicing equation, a detailed knowledge of the vertical structure of the target cloud is required. Because this knowledge does not exist, an infinite number of cloud height solutions exist for undetermined finite cloud thicknesses. Because the “true” cloud heights in this study are taken from high vertical resolution lidar measurements, differences between the “true” heights and simulator heights are expected to be non-zero.

Scenes with multiple cloud layers

Another assumption inherent to the derivation of Eqn. 3 is the existence of only a single cloud layer in the target field of view. The numerator and denominator of the CO₂ slicing equation describe the radiation signature of a column containing just one cloud layer. Introducing an analogous relation for multiple cloud layers creates a similar situation to the IR window BT method; there aren't enough inputs to a unique cloud height solution. Baum and Wielicki (1994) found that errors in retrieved heights stemming from this assumption are minimized by choosing channels for ν_1 and ν_2 whose weighting functions peak highest in the atmosphere, while still providing adequate SNR at the cloud altitude. This is implemented in the MODIS collection 5 routine by attempting convergence in Eqn. 3 using successively more opaque channel pairs (Menzel et al, 2008). If each of the three channel combinations fails to retrieve a cloud height between the surface and tropopause, the IR window brightness temperature method is used.

Signal to noise ratio issues

Although the CO₂ slicing technique was developed to correct for errors in retrievals of optically thin clouds, it can also suffer from low signal-to-noise ratios (SNR) in the LHS of Eqn. 3. If the target cloud is extremely optically thin or the radiative contrast between the cloud and underlying surface is very small, the differences between the measured and estimated clear radiances become small. In these cases, instrument measurement and ancillary data uncertainties have more of an effect on cloud height retrievals. Typical cloud masks for narrow band cloud height retrievals are not as sensitive to clouds with very low optical depths because their cloud masks use the difference in brightness temperature

between the target FOV and a known nearby clear FOV. These differences in brightness temperature will be below the instrument noise level for clouds with very low optical depth. This experiment utilizes collocated lidar measurements, which are much more sensitive to thin clouds. To reduce errors from this effect, FOVs are filtered to where the lidar retrieves optical depths of greater than 0.1.

Errors in ancillary data profiles

Employing the forward model approach to acquiring the estimated cloud-cleared radiance values requires an *a priori* knowledge of temperature and absorbing gas concentration profiles. This is source of uncertainty is unavoidable, but these errors are decreasing with increasing model and reanalysis skill. As mentioned above, clouds with low optical depths will be affected most by these uncertainties because of the resulting low SNR. Menzel et al. (1992) show that for large positive errors of in surface temperature, cloud heights are retrieved lower in the atmosphere, and the opposite for large negative errors. Errors in surface temperatures are generally small (less than 5°C) and the carbon dioxide channels are more sensitive to the upper atmosphere than the surface, so uncertainties resulting from errors in surface temperatures are assumed to be small. Zhang and Menzel (2002) found that the CO₂ slicing technique is less sensitive to uncertainties in surface emissivity than for errors in surface temperature. These uncertainties had a negligible effect for scenes containing optically thick clouds.

Errors may also come from the atmospheric temperature profiles. Errors from erroneous layer temperature in the lower troposphere are limited by selecting opaque channel combinations, so the emitted radiation from the lower troposphere is absorbed and emitted at

layers with more reliable temperatures. For layers near clouds of interest, Menzel et al (1992) finds that the error in retrieved cloud pressure due to temperature errors is inversely proportional to the temperature lapse rate at the cloud level.

Inadequate knowledge of measurement SRFs

Any space-bound instrument undergoes pre-launch testing to ensure that its spectral response functions are well characterized. This does not mean, however, that the SRFs will not change over time as the measurement filters and mirrors age. Tobin et al. (2006) (hereafter referred to as T06) compared narrow band MODIS-Aqua and hyperspectral AIRS brightness temperatures for two days of collocated observations. It was empirically discovered that shifts to the MODIS spectral response functions of 15.0nm, 15.5nm, and 20.2nm were required to explain the differences in observed brightness temperatures for MODIS-Aqua bands 34, 35, and 36, respectively. Zhang et al. (2005) used these new SRF values when analyzing two granules of MODIS measurements over tropical and mid-latitude regions. They found that using the response function shifts improved cloud height retrievals in the mid-latitudes, but the results were mixed in the tropical areas. The T06 SRF shifts cause the largest changes in cloud detection and height for combinations including band 36, which is the most opaque and most highly shifted MODIS CO₂ slicing band. This band is most sensitive to very high clouds, so it is not surprising that a more accurate knowledge of its SRF increases its skill in retrieving cloud amounts and heights of high clouds. The sensitivity of CO₂ slicing to differences in measurement and forward model response functions is tested in this study.

4. Instruments and tools

This experiment makes use of a variety of instruments and remote sensing tools. This chapter introduces the instruments and tools used in this investigation

4.1 AIRS

To accurately simulate the radiance observed by one instrument with another instrument by means of spectral convolution, the measurement instrument must be well calibrated and have numerous spectral bands in the range of the simulated instrument. The Atmospheric InfraRed Sounder (AIRS) is a 2378-channel grating spectrometer that provides hyperspectral IR radiances with wavelengths between 3.7 μm and 15.4 μm . The AIRS was launched on the Aqua Earth Observing System (EOS) in May of 2002 with a sun-synchronous polar orbit at the head of NASA's A-train satellite constellation. The AIRS is designed for high vertical resolution atmospheric sounding and provides 1km atmospheric layer temperatures to within 1K of the true temperature. The AIRS has a nadir ground footprint of 13.5km and a nominal resolving power $\lambda / \Delta\lambda$ of 1200. Viewing geometry causes FOVs to stretch to ellipses at large scan angles (Aumann et al. 2003). This causes signal redundancies near the edge of the 99° scan track, but does not affect this study because the collocated CALIOP FOVs are always close to the nadir AIRS fields of view. The AIRS uses an echelle reflective grating design, which separates upwelling radiation into high spectral resolution (0.5-2.0 cm^{-1}) orders, which are measured by the detector arrays. These extremely well calibrated (Strow et al. 2003) hyperspectral observations provide the capability to simulate narrow band instruments by convolution the narrow band spectral response functions with the AIRS observations.

4.2 CALIOP

The CALIOP (Cloud Aerosol Lidar with Orthogonal Polarization) measures attenuated backscatter amounts as a function of height at 532nm and 1064nm in a single, near-nadir track (Vaughan et al. 2004). CALIOP was launched in April of 2006 aboard the CALIPSO (Cloud-Aerosol Lidar and Infrared Pathfinder Satellite Observations) and is part of the A-Train constellation, trailing Aqua by approximately 75 seconds. CALIOP provides an independent cloud top height reference, cloud optical depths, and cloud phase. The ability of CALIOP to produce high vertical resolution backscatter retrievals results from the timing system of the active instrument's detectors. Analog voltages of the detectors measuring reflected radiation are sampled at a rate of 10MHz, which corresponds to a vertical resolution of 30m. At altitudes above 8.2km, returns are averaged to 60m in vertical resolution. The horizontal resolution of CALIOP is 333m as determined by the pulse rate of the laser. The 532nm laser is polarized so that CALIOP can distinguish between cloud particle phases using information from measuring the polarization of reflected incoming radiation (Vaughan et al. 2004).

In this experiment, each scene selection requirement is handled with the lidar in order to keep the CO₂ slicing algorithm independent from the scene selection. This decreases uncertainties due to any biases from AIRS and ancillary profiles in the production of simulated cloud top heights and isolates the differences from cloud selection in the algorithm.

4.3 HIRS/2

The HIRS/2 (High Resolution Infrared Sounder version 2) instrument measures radiation from a low earth polar orbit in 20 narrow band channels. The HIRS/2 is a cross-track scanning radiometer with a ground footprint of 17.7km. Because of the instrument's orbital speed and the cross-scanning design, the centers of HIRS/2 footprints are spaced 42km apart in the along-track direction (NOAA TOVS/ATOVS). This means the HIRS/2 does not measure radiances for the 24km of earth-scene between along-track FOVs. The HIRS/2 instruments house 19 infrared bands that, in collaboration with other TOVS instruments, have the capability to retrieve temperature and moisture profiles as well as surface temperature, cloud height and. The single visible band retrieves albedo and creates mosaics of the day side of earth (NOAA TOVS/ATOVS). All versions of the HIRS/2 instrument have 4 channels (bands 4-7) that are used to retrieve tropospheric cloud heights using CO₂ slicing. HIRS instruments have been observing upwelling radiation in the 15 μ m absorption region since the design's first launch in 1975 aboard the Nimbus 6 satellite. Because of its long observational record, HIRS/2 instruments have been used in previous studies of cloud climatologies, most notably the UW Pathfinder project (Wylie et al. 2005) mentioned in the introduction section. In this experiment, AIRS radiance measurements are convolved to the SRFs specified before launch from the HIRS/2 instruments aboard the HIRS/2 NOAA-06 (HIRS06) to NOAA-14 (HIRS14) satellites to provide simulated heights for each set of response functions. This allows the experiment to observe differences in cloud heights retrieved for the same radiance and ancillary inputs while using the spectral response functions from all instruments used in the UW Pathfinder study.

4.4 MODIS

The MODerate Resolution Imaging Spectroradiometer (MODIS) is a 36-channel narrow band radiometer currently aboard two polar orbiting NASA satellites. Nearly identical copies of the MODIS instrument fly aboard the EOS-AM Terra (launched Dec 18, 1999) and EOS-PM Aqua (launched May 4, 2002). MODIS's 36 spectral bands provide a wealth of information to scientists studying Earth's surface and atmospheric processes from phytoplankton and surface imaging in the visible bands to cloud heights and surface temperatures in the infrared bands. The MODIS instruments have four channels (bands 33-36) with ground footprints of 1km that are modeled after the CO₂ slicing channels from the HIRS/2 design. As does HIRS, MODIS employs a cross-track scanning technique for radiance measurements (Barnes et al. 2003). Unlike HIRS, the MODIS instrument design takes into account the orbital speed and finite time it takes to perform a cross-track scan. An orbital ground speed of 6.78km/s and a cross-track scan time of 0.676s implies that there are 9km of missed earth-scene between successive along-track FOVs. To avoid missing this data, 10 nearly identical detectors are aligned in the along-track direction for each NIR channel. Therefore, no data is missed and the MODIS can obtain global coverage in just two days. MODIS represents the next generation of narrow band infrared radiometers and could be included in future cloud climatology studies. In this study, cloud top heights are simulated for the SRFs belonging to the MODIS instrument aboard EOS Aqua.

4.5 Forward Model/LBLRTM

As mentioned in the introduction to CO₂ slicing, estimation of the clear sky radiances I_{clear} and values in the RHS of Eqn. 3 can come from interpolation of retrievals from nearby

clear fields of view. This is the method implemented by Wylie and Menzel (1999) in their 8-year climatology of cloud height and amounts using HIRS/2 instruments. Because the CALIOP lidar is used to generate all scene selection properties, only AIRS FOVs that co-align with the CALIOP ground track can be used for cloud height retrievals in this study. This limits candidate AIRS scenes to near-nadir views only. Employing the interpolation method in this situation would require interpolating across hundreds of kilometers, so the estimate of the cloud-cleared radiance and the values on the RHS of the CO₂ slicing equation must be computed directly with a forward radiative transfer model.

Increasing reanalysis model skill over the last 20 years allows researchers to use a forward model to accurately estimate upwelling radiance in a cloud-cleared column with increasing accuracy. There are two basic categories of forward models: line-by-line and fast models. The MODIS collection 5 CTH retrieval algorithm uses the Pressure Layer Fast Algorithm for Atmospheric Transmittances (PFAAST) to calculate cloud-cleared upwelling radiances at each designated atmospheric layer (Menzel et al. 2008). PFAAST is a fast model because rather than performing radiative transfer on monochromatic radiances and convolving the results, it convolves the radiances at each layer and then performs the radiative transfer (Hannon et al. 1996). With close to 2 million wavelengths required to resolve the fine structures of individual absorption/emission lines over the range of the MODIS and HIRS/2 carbon dioxide absorption bands, this results in a very large difference in total computation time while losing only a small amount of accuracy. Fast forward models like PFAAST are required for applications with large amounts of data or near-real time demands, but lack the flexibility required to simulate multiple instrument SRFs, as is done in this experiment.

In this study, the Line-by-Line Radiative Transfer Model (LBLRTM) is used to compute monochromatic radiances and optical depths at each potential retrieval layer in the atmospheric profile. Based on an earlier line-by-line model FASCOD (Clough et al. 1981), LBLRTM provides a flexible but computationally expensive method of supplying the CTH algorithm with accurate clear sky radiances and optical depths (Clough et al. 1992). The LBLRTM performs all calculations in monochromatic wavelength space, so the output may be convolved to any desired spectral response functions. The computational requirements of a line-by-line model are not an issue with this study, as there are no temporal or global processing demands as in a NWP or GCM setting. While LBLRTM itself is extremely accurate, its output is only as accurate as the ancillary model profiles it uses as inputs.

4.6 Ancillary Profiles

Inputs to the LBLRTM forward model are generated from NCEP's $2.5^\circ \times 2.5^\circ$ Global Data Assimilation System model profiles (Kanamitsu et al. 1991). The GDAS layers range from 1000 to 10mb, supplying reanalysis values of surface temperature and pressure layer altitudes, temperatures, and H₂O and O₃ gas concentrations. Other absorbing gas concentrations are produced by LBLRTM from molecular scatter properties tables. Because non-negligible absorption occurs in the upper stratosphere and mesosphere, profiles of absorbing gases for six standard atmospheres are supplied by the AFGL Atmospheric Constituent Profiles (Anderson et al. 1986) between the range of the GDAS profiles and 120km. Profiles are then interpolated to the same 101 pressure levels as used by the MODIS collection 5 algorithm before forward model computation.

5. Experiment and algorithm design

This chapter explains the experimental design and implementation. After explaining the method of integrating retrievals from multiple sensors the details of the experimental strategy are given in full.

5.1 Collocation

To reliably use data products from multiple satellites, it is best to find where their ground footprints overlap or where the distance between them is a minimum. This process is called collocation. This study uses collocated AIRS and CALIOP products, as well as GDAS ancillary profiles that have been collocated with AIRS. CALIOP profiles are collocated with AIRS FOVs if their ground footprints fall within an AIRS ground footprint. The details of the AIRS/CALIOP method of collocation are explained in Nagle and Holz (2009) are not considered to be central to the science objectives of this paper. Because the distance between AIRS footprints is small compared to the GDAS grid spacing, the AIRS/GDAS collocation simply selects the nearest GDAS location to each AIRS scene of interest.

At near-nadir FOVs, the AIRS footprint is approximately 13.5km in diameter. The CALIOP footprint is considerably smaller than the AIRS footprint, at only about 80 by 330 meters. Consecutive CALIOP scenes are also centered just 330 meters apart, so there are many CALIOP profiles within each AIRS field of view (Vaughan et al. 2004). The large differences in footprint diameter and spacing are convenient, as they allow a more stringent check to the assumption that the AIRS field of view is uniform. CALIOP profiles that fall within an AIRS footprint are averaged to create a single CALIOP product value for each individual AIRS footprint. This ensures that the CALIOP retrievals used for scene selection

are representative of AIRS instrument's field of view. CALIOP scenes located within an AIRS field of view are not weighted based on their distance from the center of the AIRS scene. Weighting is not considered to be necessary because, as discussed in the Scene Selection section below, most of the CALIOP products used in this algorithm are required to be uniform across the entire AIRS field of view. Because there is no sub-FOV AIRS information, it must be assumed that across track variations in target clouds are small and disappear in inter-instrument height comparisons for identical cloud scenes. AIRS scenes are also collocated with interpolated GDAS $1^\circ \times 1^\circ$ grid boxes to provide the nearest ancillary model profiles. After these collocations have been performed, the data is ready to be used to retrieve cloud top heights using CO₂ slicing.

5.2 Cloud top height simulator algorithm

As mentioned at the end of the introduction, the strength of this experiment lies in the strategy of simulating narrow band instrument CO₂ slicing cloud heights by spectral convolution of measured AIRS radiances. Measurements from AIRS constitute the only measured radiances in this study. Because each instrument's simulated heights are generated for the exact same target scenes, the effects of spectral response functions on retrieved heights may be separated from other sources of error such as differences in footprint, quality of ancillary data, and differences in the distributions of target scene properties (layer temperatures and true cloud heights and thickness). The details of the simulator algorithm are explained in this section.

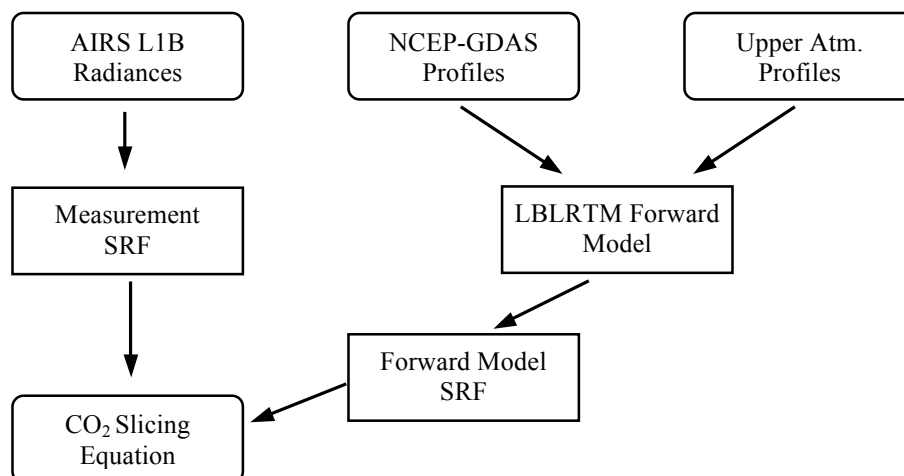


Figure 3: Simulator algorithm flowchart. AIRS radiance observations are convolved to the measurement SRFs, while LBLRTM uses profiles to estimate monochromatic clear sky radiances, which are then convolved to the forward model SRFs. Convolved radiances are then inputted to the CO₂ slicing equation to retrieve a cloud height. This process is repeated for each FOV and each simulated instrument.

The simulator algorithm is summarized in Figure 3. For each FOV, measured radiances from AIRS are convolved to the SRFs of the first simulated instrument. Collocated GDAS and AFGL profiles are then passed to the forward model (LBLRTM), which calculates a clear sky gaseous optical depth for each layer at each monochromatic frequency. The monochromatic layer to TOA transmittances are calculated through radiative transfer and a linear-in-tau (LIT) radiance correction as implemented in the computation of LBLRTM radiances from Clough et al. (1992). These monochromatic radiances and transmittances are then convolved to a special joined SRF that combines the SRFs of AIRS and the SRFs of the simulated instrument. Because the AIRS SRFs are included in the computation of convolved measured radiances and transmittances, the convolution correction implemented in T06 is unnecessary. The measured radiances and cloud-cleared radiances and transmittances are then applied to the CO₂ slicing equation. Ancillary layer temperatures determine the profile of blackbody radiances. After a height is retrieved for the SRFs the simulated instrument, the

exact same inputs are used to compute a cloud height for the next simulated instrument, and so on until all sets of SRFs have been used. The algorithm then moves to the next cloudy AIRS scene and repeats the retrieval process.

Operationally, the left and right hand sides of the CO₂ slicing equation are computed separately. The integrals on the right hand side are calculated for the surface to each layer in atmosphere, creating a vector of values for the RHS. This is done because the potential cloud heights are the upper bounds on the integrals. The retrieved cloud top height is the altitude that corresponds smallest difference between the left hand side and the right hand side of the CO₂ slicing equation. Potential retrieval layers are limited to altitudes between 3.5km and 18km to eliminate erroneous solutions resulting from irregular GDAS retrievals and the stratospheric temperature inversion, respectively.

5.3 Radiance bias correction

A clear sky radiance calculation is used to account for systematic errors in the estimated clear sky radiances retrieved with the forward model LBLRTM. These biases may result from inaccuracies in the GDAS and AFGL ancillary profiles, errors coming from GDAS grid boxes being far from the clear scene, or the fact that not all absorbing gas constituent profiles can be taken into account in the GDAS model profiles. Errors resulting directly from LBLRTM are assumed to be very small, as LBLRTM is a line-by-line algorithm and is extremely accurate (Clough et al. 1992).

For each CO₂ absorption region band in each simulated instrument, TOA radiances for all clear scenes are calculated for each day and compared to convolved radiance measurements from AIRS. The mean difference between these values is applied to the

estimated clear sky radiance at the left hand side of the CO₂ slicing equation during cloud height retrieval. This process is repeated for each set of response functions, so a separate radiance bias correction is computed for each simulated instrument.

The MODIS collection 5 and 6 cloud height algorithms employ a similar bias correction in the calculation of its cloud heights using CO₂ slicing. In the MODIS algorithm, clear scene radiances are not averaged over a single day, as in this experiment. Rather, the estimated radiances are binned to 2.5° x 2.5° grids and applied as a rolling mean for the previous 8 days (Menzel et al. 2008). Because this algorithm uses only AIRS scenes that are collocated with the single-track lidar CALIPSO, the same latitude and longitude is only viewed twice per day and there are not enough clear scenes in a given grid box to facilitate significant bias correction retrievals at a fine spatial resolution. A single, averaged value must be used for the bias correction for each day.

5.4 Scene selection

Scene selection when obtaining heights using AIRS L1B radiances is performed entirely from information retrieved with CALIPSO. For an AIRS scene to be fit for cloud height retrieval, the collocated CALIOP FOVs must produce an average between 7 and 18km in the 5km L2 cloud height product. This limits cloudy scenes to very cold clouds, which will most likely be composed of ice crystals instead of super-cooled water droplets. To further exclude water clouds, scenes are also limited to where the CALIPSO cloud phase has been determined to be ice-only. Chosen cloud scenes are also limited to latitudes that fall between 50°S and 50°N. Scenes are limited in latitude because GDAS profiles are more uncertain at extreme latitudes. Cloud scenes are not filtered by the number of layers CALIPSO retrieves

for a collocated AIRS field of view. Cloud layers are used when filtering computed cloud heights in the analysis, but not for initial scene selection. The CALIOP “Cloud Layer Fraction” must equal one for the entire AIRS field of view to lessen complications from cloud edges. The collocated CALIPSO scenes must also have a mean extinction quality assurance flag of 16 or less, which reduces errors resulting from inaccurate CALIOP retrievals in height analyses.

To ensure that the FOVs used in the clear sky radiance bias calculation are completely clear, only FOVs that satisfy strict requirements are used. The CALIOP cloud fraction product must be zero for each 5km averaged CALIOP profile in the AIRS scene. The AIRS field of view must also fall between 50°S and 50°N in latitude. Again, this is to reduce errors from inaccurate GDAS profiles.

6. Data sources

6.1 AIRS

AIRS L1B collection 5 geolocated radiance products were acquired from http://airs.jpl.nasa.gov/data/get_AIRS_data/ in Aug 2010 for the full days of Aug 2 and 10, 2006. An example file is “AIRS.2006.08.02.001.L1B.AIRS_Rad.v5.0.0.0.G07119073539.hdf”. Not all of AIRS’s 2378 channels are fit for scientific research. Excluded channels are noisy or exhibit radiance “popping”, among other reasons. These channels are eliminated by the “Bad_Flag” variable in the “L2.chan_prop.2003.11.19.v8.1.0.tobin.anc” channel property file acquired through person correspondence with Dave Tobin. In all, 280 AIRS channels are excluded, but only 17 of these are in the range of the MODIS bands used in this study. AIRS channels have long SRF tails, so no spectral gaps result from the exclusion of channels. The method of using joined AIRS/MODIS and AIRS/HIRS06, etc. response functions eliminates the need for convolution corrections to account for missing AIRS channels.

6.2 CALIOP

CALIOP lidar products were retrieved from the PEATE data archive at the SSEC in Madison, WI. Version 1 L1B files such as “CAL_LID_L1-Prov-V1-10.2006-08-02T00-31-26ZD.hdf” were used for total attenuated backscatter files. Level 2 files came from V2 333m, 1km, and 5km Cloud Layer and 5km Cloud Profile files, also from the PEATE archive. CALIOP files were acquired in Aug 2010 for the days of Aug 2 and 10, 2006. Relevant lidar products from these files are collocated with AIRS radiances. The lidar spatial resolution is reduced and the two sets of retrieval products are merged into a single file.

6.3 GDAS

Ancillary surface temperature and layer pressure, geopotential height, relative humidity, temperature, and ozone concentrations are taken from 6-hourly NCEP GDAS reanalysis grids at $1^\circ \times 1^\circ$ spatial resolution. These files are collocated with AIRS latitudes and added to the AIRS/CALIOP match files.

6.4 AFGL

The Air Force Geophysics Laboratory (AFGL) atmospheric constituent profiles used as ancillary data above the range of the GDAS reanalysis profiles originated from the Anderson et al. (1986) study. Concentrations were taken directly from the paper and used as a lookup table by latitude and day of year. The AFGL constituent values are stacked on top of the GDAS reanalysis layers and the entire profile is interpolated to the layers used by the PFAAST fast algorithm, which is used by the MODIS collection 6 cloud height algorithm (Menzel et al. 2008).

6.5 HIRS/2 SRF

The HIRS/2 spectral response functions used in this study are the original pre-launch measured SRFs from

<http://www.orbit.nesdis.noaa.gov/smcd/spb/calibration/hirs/srf/hirssrf.html> in Aug, 2010.

HIRS/2 response functions from the NOAA06 through NOAA14 were downloaded and pasted into separate files for each spectral band. These response functions were not altered during the course of this study.

6.6 MODIS SRF

In this study, spectral response functions labeled as “Aqua” or “unshifted” are the results of pre-launch calibration of the MODIS instrument on EOS Aqua. The unshifted response functions may be downloaded from http://www.ssec.wisc.edu/~paulv/Fortran90/Instrument_Information/SRF/Data_Files.html. Response functions for each of 10 detectors per band were linearly averaged to create a single response function per MODIS-Aqua spectral band. The T06 study used the same averaging procedure. All shifted response functions used for this study were computed from the pre-launch MODIS-Aqua response functions acquired from the above web address. Linear shifts were applied to the averaged SRFs for each band in $\frac{1}{2}$ increments of the shift amounts listed in T06. Shifts ranged from 0 to 2 times the T06 amounts, resulting in five distinct versions of the Aqua SRFs.

7. Results

7.1 Selected scene characteristics

From the two days of Aug 2 and 10, 2006 and the scene selection described earlier, CO₂ slicing cloud height retrievals are made for a total to 3,687 AIRS cloud scenes.

Distributions of CALIOP-retrieved top layer optical depth and height are shown in Figure 4.

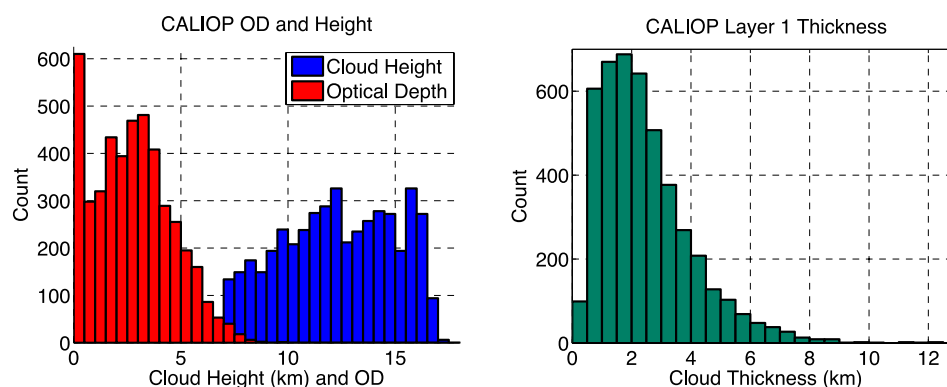


Figure 4: CALIOP cloud height, optical depth, and top layer thickness for all cloudy scenes used to retrieve cloud heights. Scenes with CALIOP optical depths smaller than 0.1 have been excluded.

The first noticeable feature in Figure 4 is the number of FOVs for which CALIOP retrieved an optical depth of less than 0.5. If scenes containing clouds with CALIOP optical depths less than 0.1 are included this artifact shifts closer to zero and peaks at around 0.005. This could be due to the CALIPSO retrieval mistakenly identifying thin aerosol layers with clouds layers, an error in the CALIPSO parameterization for scattering phase functions, among other things (personal correspondence with Bob Holz). Clouds with small optical depths do not violate any of the CO₂ slicing assumptions, but they can cause large uncertainties due to low signal to noise ratios in the LHS of the CO₂ slicing equation, as described in Chapter 3. There are relatively few AIRS scenes containing top layer clouds with optical depths greater than 6. This is chiefly due to the attenuation of the CALIOP lidar signal within the cloud, but also

includes effects the definition of what constitutes a distinct cloud layer. Under the single scattering regime, the CALIOP can only measure optical depths of about three. However, multiple scattering events effectively add energy to the system, allowing the CALIOP to “see” farther into the cloud. The first cloud layer (viewed from space) is defined as the portion of the atmosphere between where the lidar measures a distinct cloud backscatter signal and the altitude where that signal diminishes to clear-scene levels. To define a second cloud layer, the backscatter signal must again rise to cloud levels, but the distance between the bottom of the first layer and the start of the second cloud layer must be greater than 200m. If the distance between these two altitudes is less than 200m, the portion of the atmosphere containing the second increase in backscatter signal is considered to be a part of the first layer. The total column optical depth is often much larger than what is shown in Figure 4 because of the inclusion of underlying optically thick water clouds. Figure 4 also shows that the CALIOP cloud height distribution is fairly flat over the two days, with a lower bound of 7km as defined by scene selection. This presents a collection of cloudy scenes that represent many different physical atmospheres. The cloud thickness portion of Figure 4 shows that only a few (3.1%) selected scenes contain clouds thicker than 6km, which are products of tropical deep convection. Most of the selected FOVs, however, contain geometrically thin cirrus clouds with optical depths less than 3, which are the target of this study.

7.2 Case study of retrieved heights

In Figure 5, simulated heights using MODIS-Aqua spectral response functions are plotted in red over the corresponding CALIOP total attenuated backscatter profiles.

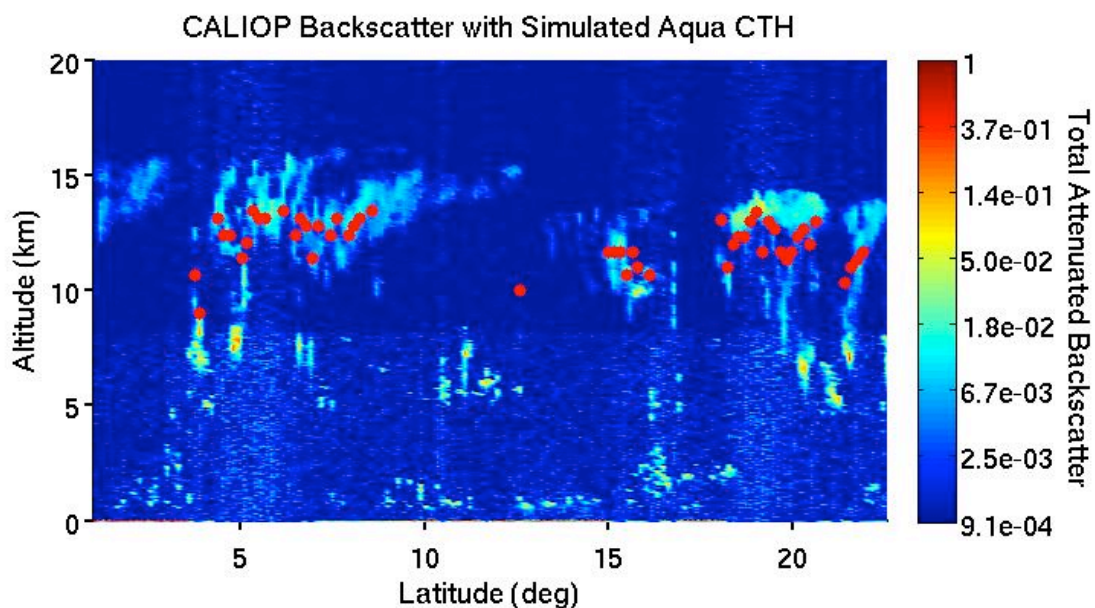


Figure 5: A single granule of CALIOP total attenuated backscatter profiles with simulated heights for MODIS-Aqua bands 36/35 as red dots. Higher backscatter measurements correspond to more reflective areas of the atmospheric profile.

Chapter 3 explains that CO₂ slicing algorithms tend to produce heights that correspond to where the cloud optical depth is equal to one when viewed from space. Therefore, a cloud with high extinction will produce a height that is very near the physical cloud top and a cloud with low extinction will produce a height closer to the middle of the cloud. The optically thin clouds between latitude intervals 5°-8° exemplify this property of the CO₂ slicing method.

The retrieved height for HIRS06 at 12.5° show one weakness of CO₂ slicing algorithms. Here, optically thick clouds at 5km underlie optically thin cirrus at 15km, causing large errors in the upper cloud's altitude. Baum and Wielicki (1994) find that with the existence of a lower opaque cloud, cloud heights for the upper thin cloud are retrieved lower in the atmosphere than they would be without the presence of the lower cloud. The CO₂

slicing equation is formulated for columns with a single cloud layer or for scenes with opaque upper clouds, which is not the case at this location.

CTH retrievals for columns that do not violate the assumptions inherent to Eqn. 3 behave as expected. Cloudy column at latitudes 18° to 19° have little underlying cloudiness, so heights are retrieved around the radiative mean of the cloud. While there is significant low cloudiness at latitudes at 16° and 21° , the upper clouds are thick, so these effects are limited.

As explained in Chapter 4, HIRS/2 and MODIS each have 4 channels in the CO_2 absorption band, but their channel numbers do not match. For convenience in this study, channel combinations are reported as band combination 1, 2, and 3, which correspond to MODIS-Aqua bands 36/35, 35/34, and 35/33 and HIRS/2 bands 4/5, 5/6, and 5/7, respectively. This assignment is summarized in Table 1.

Table 1: Labeling of MODIS-Aqua and HIRS/2 channel combinations as v_1/v_2 in Eqn. 3

	Band Combination 1	Band Combination 2	Band Combination 3
MODIS-Aqua Channels	36/35	35/34	35/33
HIRS/2 Channels	4/5	5/6	5/7

7.3 Effects of radiance bias correction

As mentioned earlier, this study employs a clear sky radiance bias correction to mitigate systematic errors in the estimated clear sky radiance for each cloudy field of view. Radiance bias corrections of 0.3541, -0.1992, -0.6966, -0.9798 $\text{mW}/(\text{m}^2 \text{ sr cm}^{-1})$ are computed using the procedure explained in Chapter 5 for bands 33 through 36, respectively, and added to the estimated clear sky radiance found by the forward model LBLRTM for Aug 2. The direct effects of this bias correction are shown in Figure 6, where histograms of the differences between the simulated heights and the retrieved cloud heights from CALIOP are

displayed for each of channel combinations 1 (red) 2 (blue), and 3 (black), with corresponding means plotted as vertical lines.

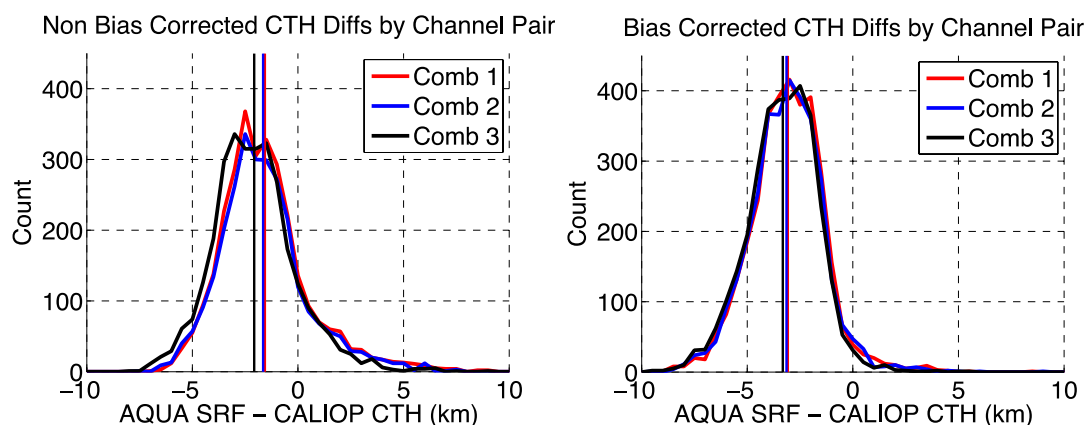


Figure 6: Cloud height differences from the CALIOP lidar for non-bias corrected (NBC) and bias corrected (BC) for band combinations 1 (red) 2 (blue) and 3 (black). Locations of distribution means are plotted as vertical lines.

In these distribution plots, a negative value corresponds to the heights simulated using the MODIS-Aqua SRFs retrieved lower in the atmosphere than the CALIOP lidar. These two plots show a few important effects of the radiance bias correction. First, the cloud height difference distributions are relatively similar for all three band combinations, even though they are each sensitive to different parts of the atmosphere. Also, the addition of the clear radiance bias correction has a similar affect for each band combination, shifting the distributions lower in the atmosphere.

As explained in the introduction, CO₂ slicing cloud heights should not exceed heights retrieved using lidar backscatter measurements. In the non-bias corrected histograms on the left, about 15% of retrievals produce these non-physical solutions (seen as differences greater than zero). The bias correction largely eliminates these over estimates, shifting the entire distribution toward lower heights with an emphasis on scenes with problematic retrievals.

While it is true that this increases the distance between the true cloud height and the simulated heights, the bias corrected retrievals are more representative of how the CO₂ slicing equation should perform, given correct ancillary data and a perfect forward model.

The effect of the clear sky radiance bias correction is felt similarly across all simulated instruments. Cloud heights computed with a bias correction are, on average, between 1.3km and 1.9km lower in the atmosphere than the heights computed without a bias correction.

Unless otherwise noted, all cloud heights reported for the remainder of this paper have been computed with a similar but separately calculated clear sky radiance bias correction explained in the Radiance Bias Correction section in Chapter 5.

7.4 Comparison to MODIS collection 6 cloud height product

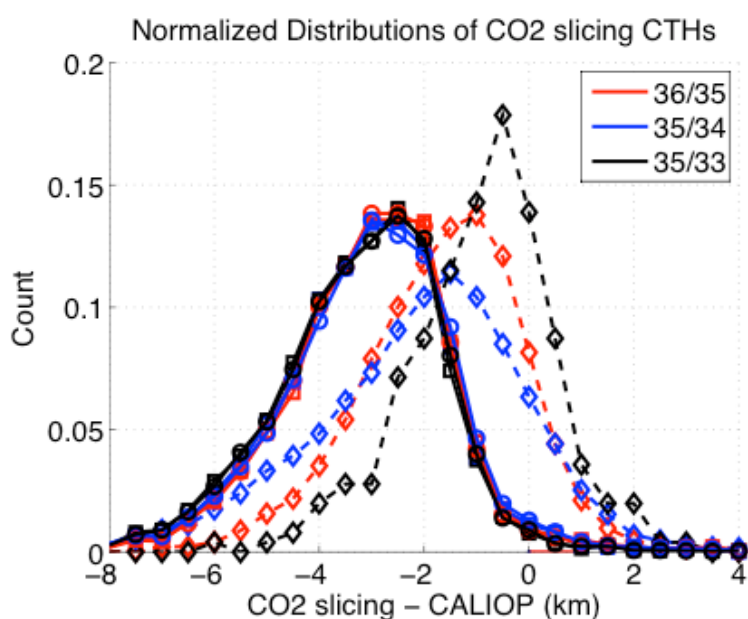


Figure 7: Normalized distributions of differences between CO₂ slicing cloud heights and the CALIOP cloud height. MODIS collection 6 CTHs and heights simulated for MODIS-Aqua are shown with as a dashed line with diamonds and squares, respectively. Circles represent the simulated case where the forward model and measurement SRFs have been shifted by the amounts found by Tobin et al (2006).

The performance of the CO₂ slicing simulator algorithm as compared to the MODIS collection 6 cloud height product is shown in Figure 7. The distributions have been individually normalized to account for the large difference in sample sizes resulting from differences between the ground footprint of MODIS and AIRS. The simulated instruments are consistently lower in the atmosphere (farther to the left) than the MODIS collection 6 heights. While MODIS collection 6 produces heights that are more closely centered around the truth cloud height (zero line), there are a lot of scenes for which the collection 6 height is retrieved above the truth cloud height, which is not expected from the CO₂ slicing equation.

The large difference between the simulator heights and the MODIS collection 6 heights come from a variety of different sources. These include the method of applying a clear sky radiance bias correction, FOV size, an inaccurate knowledge of the MODIS instrument's measurement SRFs, and others.

7.5 Differences from CALIOP lidar observations

To observe how the simulated cloud heights compare to the physical cloud top heights, CTHs from the CALIOP lidar are subtracted from the calculated heights for each of the simulated instruments and displayed in Figure 8.

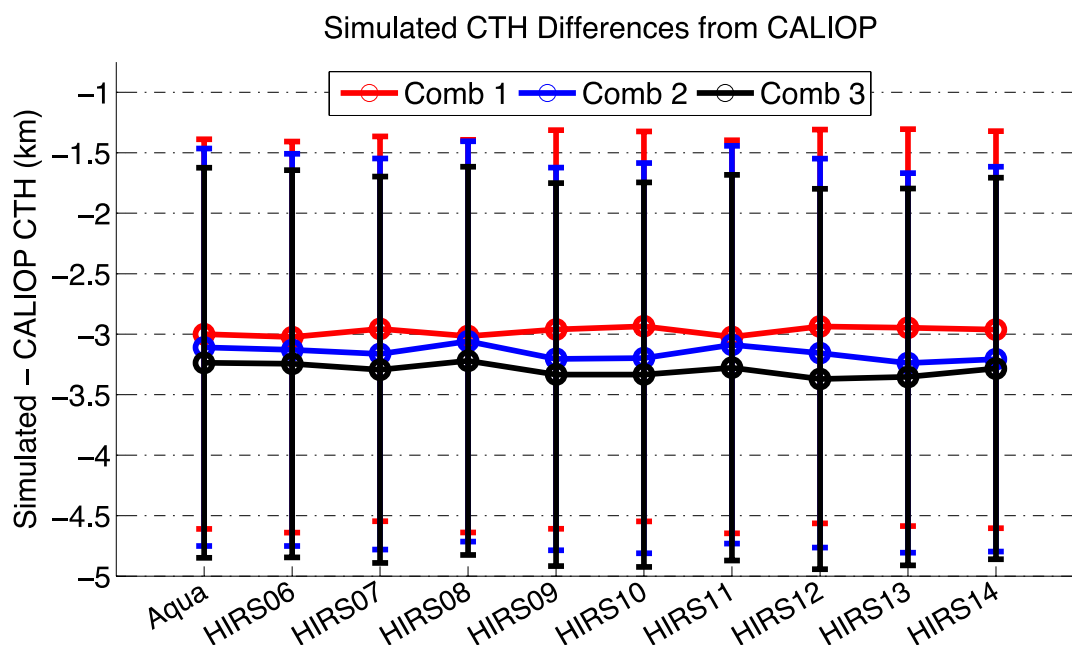


Figure 8: Simulated cloud heights as differences from the CALIOP lidar. Distribution means are again plotted as circles with 1 standard deviation designated by the bar ends.

The distributions of each CALIOP Differences of 0km and -3km correspond to the simulated height being identical to and 3km below the CALIOP height, respectively. The horizontal lines exist to further identify the locations of the means, not to imply trends across simulated instruments.

The means of the difference distributions between the simulator and lidar heights are all between 2.7 and 3.5km below the CALIOP for all band combinations. The SRF differences between simulated instruments do not have drastic effects on simulated radiances, which would cause many retrievals to be unable to converge at reasonable altitudes. Because of the locations of their weighting functions, band combination 1 is most sensitive to the upper atmosphere. This explains why band combination 1 is consistently higher than band combinations 2 and 3, which are sensitive to lower altitudes. This figure is an effective way

to show how the simulator algorithm performs versus the “true” cloud height as inferred by the lidar, but this study is concerned with the biases between simulated instruments.

7.6 Differences from HIRS06

Each difference distribution in Figure 8 has a large standard deviation, roughly 1.6km. The cloud height distributions for each simulated instrument are not computed from random, independent FOV samples; they are in fact computed for the same FOVs and are therefore not independent. Because heights for each instrument are simulated for the same cloud scenes, heights simulated for the same FOV are likely to exhibit similar effects if they have a systematic error coming from a bad ancillary profile, an underlying cloud layer, or some other violation of the the CO₂ slicing method assumptions. For example, a FOV with a temperature profile error that causes a large negative bias for one simulated instrument is likely to cause a similar bias for other simulated instruments because the ancillary data used for a particular cloud scene is identical across simulated instruments.

To eliminate these effects, heights computed for HIRS06 (chosen arbitrarily) are subtracted, scene-by-scene, from heights simulated for all other instruments. Because heights are subtracted for identical FOVs, effects from all sources except differing instrument spectral response functions are eliminated, which is the goal of this study. The results of this subtraction are shown in Figure 9.

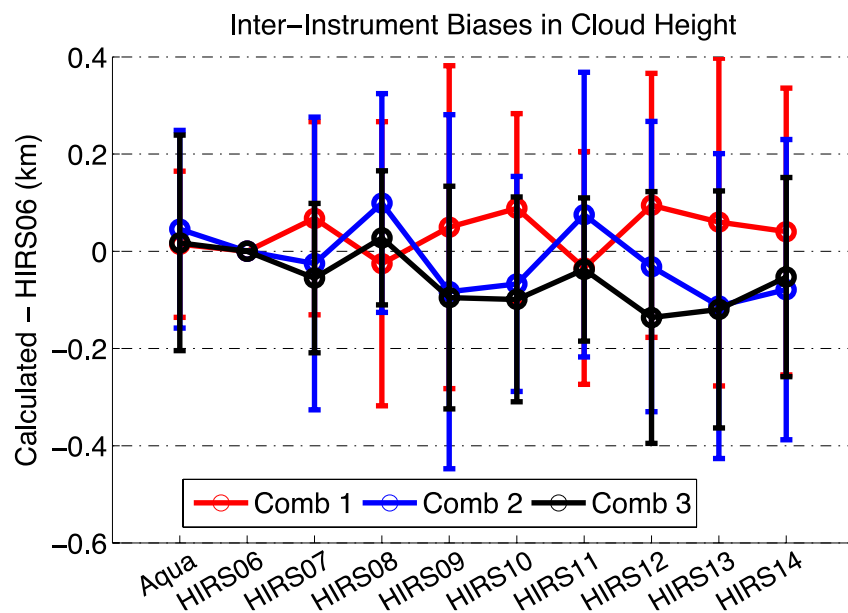


Figure 9: Inter-instrument biases in computed cloud heights using CO₂ slicing for the same cloud scenes. Differences for HIRS06 are zero for all band combinations because heights for HIRS06 have been subtracted scene-by-scene from all simulated instruments.

Again, band combinations are ordered red, blue, and black for most opaque to least opaque channel combinations and a value of -1km signifies that heights for that simulated instrument are 1km below the heights simulated for HIRS06. Difference distributions for all three HIRS06 band combinations are zero because identical values have been subtracted from them. This figure represents the goal of this study; to quantify the inter-instrument biases in retrieved cloud top heights using CO₂ slicing due specifically to differences in instrument spectral response functions. As seen previously in Figure 8, the scatter in mean differences between HIRS/2 instruments is small. Heights simulated with MODIS-Aqua SRFs are in family with the other instruments' heights.

7.7 Significance

It is desirable to assess the significance of the differences between these means to determine the probability that the means come from different distributions. Most statistical methods require that distributions be derived from random, independent samples and, as discussed earlier, this experiment does not satisfy those requirements. This, however, is one of the strengths of the experimental design. The scene-by-scene comparisons remove all effects other than those from differing instrument SRFs. Confidence intervals calculated with this method will tend to slightly overstate the significance of means differences, so 99% confidence intervals are taken instead of the standard 95%. Student t-tests are used to identify which cloud heights distributions are significantly different from those simulated for HIRS06, with results shown in Figure 10. The 99% confidence intervals are found to be close to 50m for each comparison. HIRS06 has been left out because its bias and confidence intervals are zero. All simulated instruments at all band combinations are found to be significantly different than the results from HIRS06.

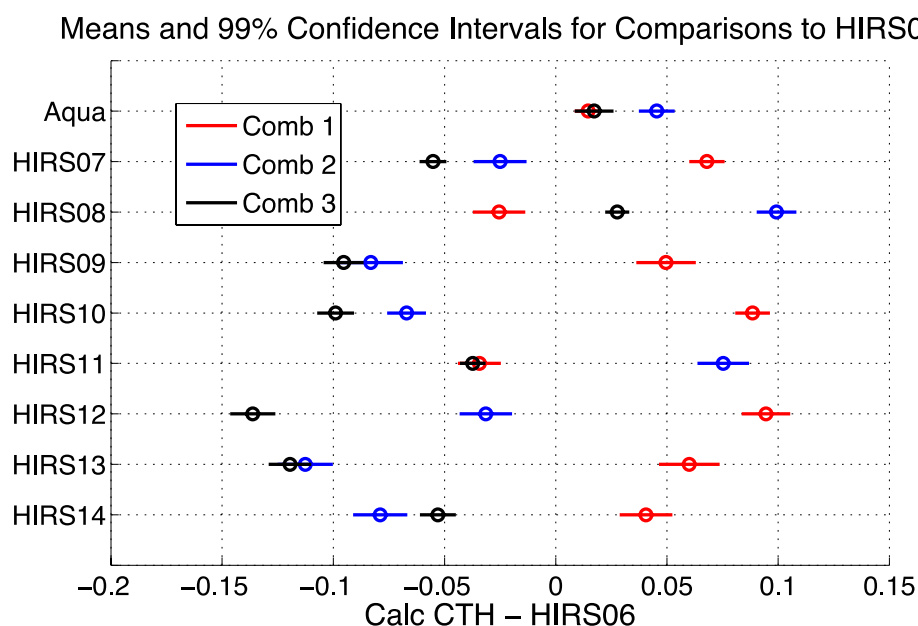


Figure 10: T-test analysis of differences between means of simulated heights compared to HIRS06. 99% confidence intervals surround the means as horizontal lines. If the confidence intervals do not overlap with zero, the simulated instrument is said to be significantly different than HIRS06.

It is also instructive to compare the differences between simulated CTHs to the commonly cited uncertainty of CO₂ slicing algorithms (including all measurement and algorithmic sources of error), which is about 30mb (personal correspondence with Paul Menzel), or about 0.75km at an altitude of 10km. While the differences between means of simulated instruments are much smaller than this value, the experimental design creates such a controlled study with few sources of differences other than spectral response functions that the retrieval uncertainty in this study is likely much less than 0.75km. Even though differences between means are within the real-world measurement noise, these are systematic biases found with SRFs being the only source of differences between cloud height retrievals for each FOV. Table 2 displays all comparisons of means. Band combinations are color coded in the same fashion as in Figure 9.

Table 2: Summary of comparisons of means. Values are calculated as “Row minus Column”. For example, Aqua minus HIRS06 for the band combination 1 is 0.013km and HIRS07 minus HIRS11 for band combination 2 is -0.110km.

	Aqua	HIRS06	HIRS07	HIRS08	HIRS09	HIRS10	HIRS11	HIRS12	HIRS13	HIRS14
Aqua		0.013 0.050 0.021	-0.055 0.072 0.074	0.042 -0.054 -0.007	-0.038 0.135 0.114	-0.077 0.117 0.116	0.052 -0.036 0.055	-0.084 0.078 0.151	-0.047 0.163 0.135	-0.026 0.125 0.066
HIRS06			-0.068 0.028 0.056	0.025 -0.104 -0.029	-0.054 0.091 0.098	-0.090 0.070 0.101	0.036 -0.082 0.036	-0.098 0.032 0.139	-0.063 0.119 0.121	-0.042 0.081 0.050
HIRS07				0.094 -0.130 -0.085	0.015 0.061 0.043	-0.021 0.044 0.045	0.105 -0.110 -0.020	-0.028 0.005 0.085	0.003 0.093 0.066	0.027 0.055 -0.006
HIRS08					-0.081 0.191 0.128	-0.114 0.173 0.131	0.010 0.016 0.065	-0.125 0.132 0.168	-0.089 0.218 0.151	-0.070 0.180 0.079
HIRS09						-0.036 -0.022 0.003	0.090 -0.165 -0.063	-0.047 -0.062 0.044	-0.009 0.029 0.023	0.012 -0.007 -0.049
HIRS10							0.127 -0.153 -0.065	-0.007 -0.037 0.040	0.023 0.052 0.021	0.048 0.014 -0.050
HIRS11								-0.135 0.113 0.104	-0.098 0.196 0.086	-0.079 0.161 0.014
HIRS12									0.034 0.089 -0.020	0.058 0.052 -0.092
HIRS13										0.021 -0.037 -0.072

7.8 Dependence on optical depth

Figure 11 demonstrates how the CTH simulator reacts to varying cloud optical depth. Simulated cloud heights are subtracted from CALIOP heights to account for correlations between cloud optical depth and true cloud altitude. MODIS collection 6 heights are again consistently higher than heights for simulated instruments, but all instruments show a trend of increasing height with decreasing cloud optical depth.

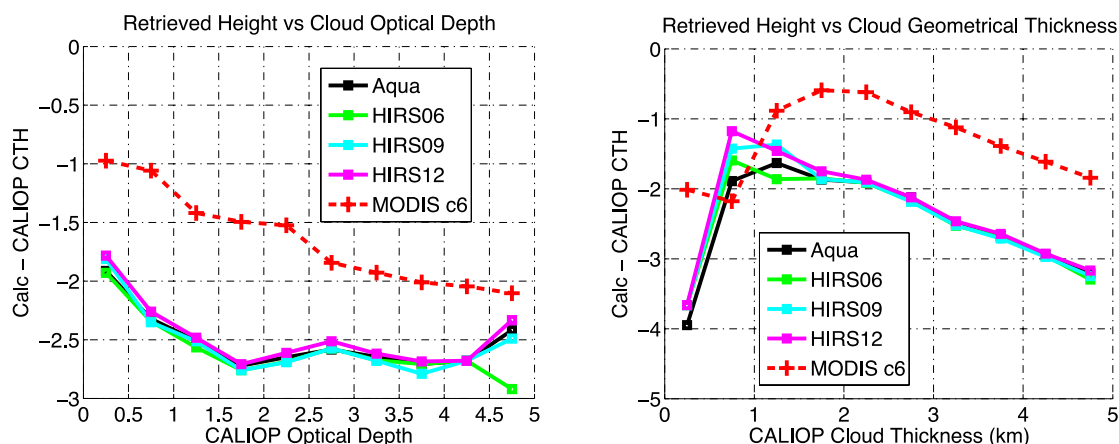


Figure 11: Dependence of all retrieved cloud heights to top layer optical depth and cloud geometrical thickness, as reported by CALIOP. Results are shown for where CALIOP retrieves single cloud layer. Heights simulated for HIRS/2 and Aqua behave similarly to the MODIS collection 6 retrievals.

It is counter intuitive to see that retrieved heights descend with increasing optical depth. Eqn. 2 suggests that the retrieval for a cloud with high optical depth will be higher than that for a cloud with low optical depth. However, this assumes the two clouds have similar extinction profiles, which may or may not be the case. The second plot in Figure 11 helps explain the trend in optical depth. It is expected that thick clouds would also have high optical depths (correlation of 0.300 for these two days), which would cause height retrievals to converge closer to the cloud top than for thinner clouds. Again, this is not observed in the data. As stated in the beginning of this chapter, the CALIOP lidar is only able to penetrate the cloud to where the optical depth is about 3. Therefore, if CALIOP retrieves a large cloud layer thickness, the cloud must be tenuous. This property, as explained in Chapter 3, causes the CO₂ slicing algorithm to produce heights farther below the physical cloud top boundary. This CALIOP sampling issue also explains the low correlation between cloud optical depths and cloud geometrical thickness of 0.300. If all clouds were considered, the correlation would be closer to unity.

7.9 Uncertainties in pre-launch measurements of SRF

Once in orbit, instrument SRFs may not be identical to the measurements made during pre-launch calibration studies. As an example, shifts of 0.8cm^{-1} (-15.5nm), 0.8cm^{-1} (-15.0nm), and 1.0cm^{-1} (-20.2nm) in MODIS-Aqua bands 34-36 can explain differences in collocated and convolved AIRS and MODIS brightness temperatures (Tobin et al, 2006). To test the sensitivity of CO_2 slicing to differences between measurement and forward model SRFs, measurement SRFs are held constant at T06 values while forward model SRFs are given incremental, linear shifts of 0.0, 0.5, 1.0, 1.5, and 2.0 times the T06 shifts from the pre-launch MODIS-Aqua SRFs. Figure 12 shows the incrementally shifted SRFs for band 34.

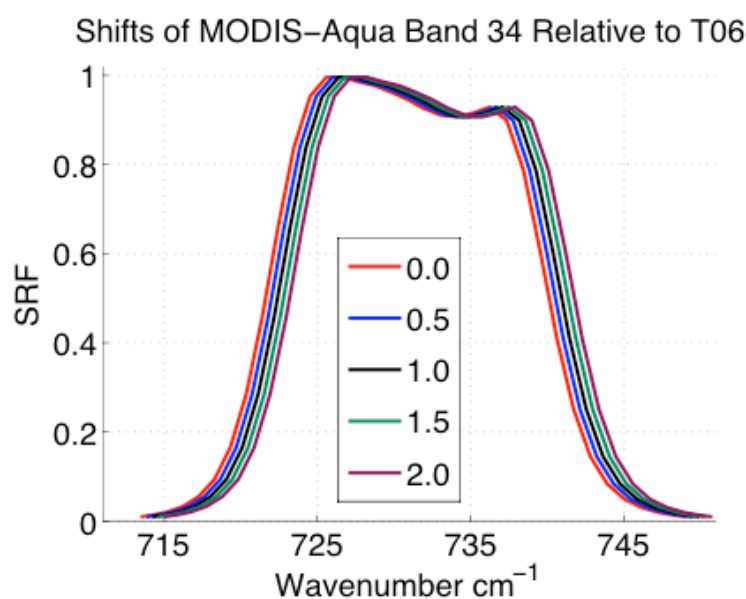


Figure 12: Incrementally shifted SRFs relative to the T06 shift amounts. The red (0.0) SRF is identical to the SRF from Figure 1, and the black (1.0) SRF is identical to the band 34 SRF from T06.

The same AIRS measured cloudy scenes were run using the cloud height simulator algorithm to determine this sensitivity. Radiance bias corrected results as differences from the CALIOP lidar are shown in Figure 13.

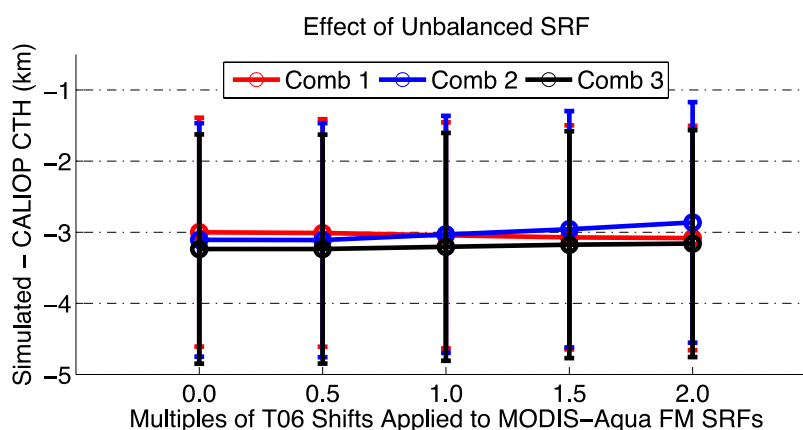


Figure 13: Effects of having incrementally shifted forward model SRFs, but constant measurement SRFs. Forward model and measurement SRFs are identical only for the 1.0 (middle) set of SRFs, which is the simulation that uses T06 shifts for the forward model and measurement SRFs.

Again, the differences resulting from the shifts are small. To eliminate effects of large standard deviations within each simulated instrument's cloud height differences, results from the 1.0 case (identical T06 SRFs) are subtracted from these simulated instruments as was done previously with HIRS06 for Figure 9. The results of this subtraction are shown in Figure 14.

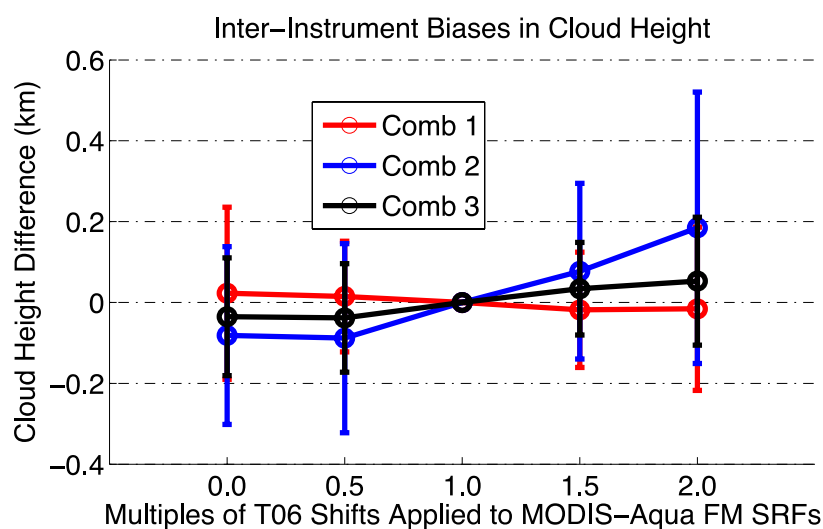


Figure 14: Direct effect of unbalanced measurement and forward model SRFs. Heights for the 1.0 (middle, T06 amounts) have been subtracted, scene-by-scene, from other retrieval distributions.

Figure 14 shows that differences in retrieved heights due to shifts in the forward model SRFs is smallest for band combination 1. This is the combination that is attempted first by the MODIS collection 6 cloud height retrieval algorithm (Menzel et al, 2008). The largest deviations from the identical SRF case occur in the 2.0 case, which is the least probable to be the truth, as the MODIS-Aqua SRFs were first measured at the 0.0 case, then empirically found to be the 1.0 case in the T06 study. Band combination 2 is the most sensitive to the unbalanced SRFs, with mean difference values ranging between -0.1 and 0.2km. The differences in how the shifted SRF cases respond to different cloud types are small and are in family with the HIRS/2 simulations, showing a lowering of heights with increasing cloud optical depth and geometrical thickness. Figure 15 shows results of t-test comparisons for band combination 1 data shown in Figure 14 with the same notation as Figure 10. Again, all simulated instruments are significantly different from the reference identical measurement and forward model SRF case.

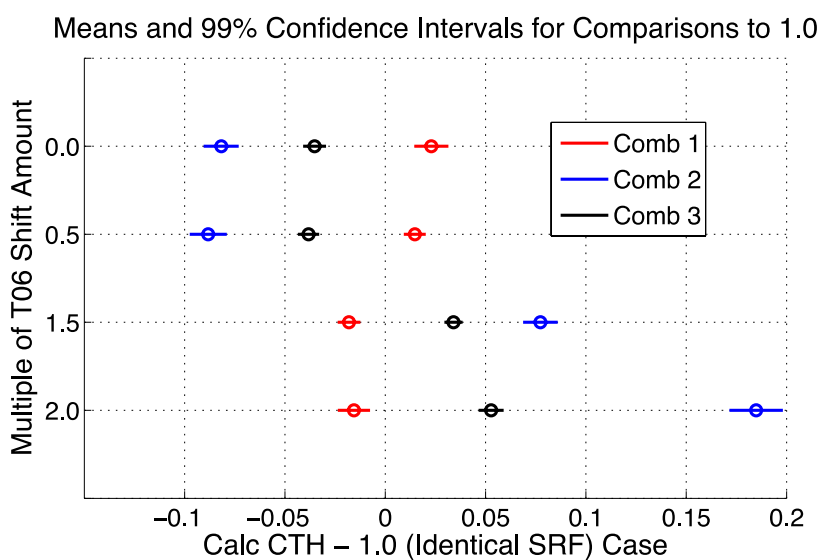


Figure 15: 99% confidence t-test intervals for the means shown in Figure 14. Comparisons are made to the 1.0 case, so this case is omitted from the figure. Each comparison of means is found to be statistically significant to 99% confidence.

8. Discussion

8.1 Summary of experiment

The goals of this research were to quantify the biases in retrieved cloud top heights using CO₂ slicing due specifically to inter-instrument differences in SRFs and to investigate the sensitivity of CO₂ slicing to cases where the measurement and forward model SRFs are not identical. A flexible CO₂ slicing algorithm was constructed to use hyperspectral, measured radiances and a line-by-line forward model to simulate narrow band radiances via spectral convolution and retrieve a cloud height. The hyperspectral nature of AIRS measurements permits the simulation of the carbon dioxide absorption band channels of any passive, narrow band instrument. Because the simulator algorithm was run using the same ancillary profiles and measured radiances across each simulated instrument, cloud height comparisons were made on a scene-by-scene basis. The spectral response functions were the only varying inputs to the simulator algorithm for a given FOV, so differences between calculated CTHs are due to differences in SRFs only.

8.2 Significance to UW Pathfinder

To observe the SRF-induced cloud height biases between instruments used in the 2005 UW Pathfinder study, cloud heights for HIRS/2 instruments aboard the NOAA06 through NOAA14 satellites were simulated for two days of nearly global AIRS radiances. The pre-launch SRFs of MODIS-Aqua were also used to retrieve CTHs. Distribution differences between simulated HIRS/2 and MODIS-Aqua instruments were found to be statistically significant, but below the error levels for typical CO₂ slicing algorithms. The

controlled nature of the experiment suggests that the uncertainties in inter-instrument biases for this study are less than that of typical operational algorithms, which must include more sources of uncertainty. The inter-instrument biases in retrieved cloud heights found in this study are on the order of 0.2 km and could affect estimates of changing cloud heights in cloud height records, though are probably not a dominant source of error. To continue a long-term cloud climatology, hyperspectral observations convolved to HIRS/2 SRFs provide the most consistent and bias-free cloud height trends.

8.3 Forward model SRF shifts

To observe CTH sensitivities to small differences between the measurement and forward model spectral response functions, SRFs for MODIS-Aqua were given linear shifts in the increments of 0.0, 0.5, 1.0, 1.5, and 2.0 times the T06 amounts. Heights were then simulated using the T06 response functions for the measurement convolution and the incrementally shifted SRFs in the forward model convolution. Using these five SRF combinations, band combination 1 is the least sensitive to SRF uncertainties, with differences between the case of identical measurement and forward model SRF of between -0.02 and 0.02km. This shows that the sensitivity of CO₂ slicing to errors in forward model SRF characterization is small for the channel combination that is preferentially chosen by the MODIS collection 6 CTH algorithm. Channel combination 2 is the most sensitive, with differences from the 1.0 case (identical measurement and forward model SRF) of between -0.1 and 0.2km for the simulated cases.

9. Future work

As an algorithm validation effort, simulated MODIS-Aqua and T06-shifted heights will be compared to collocated and averaged MODIS-Aqua collection 6 heights. For further validation, measured MODIS-Aqua radiances will also be averaged and used as $I(\nu)$ in the CO₂ slicing equation. Heights generated with radiances measured with MODIS-Aqua will be compared to averaged MODIS collection 6 heights.

Though effects from an erroneous bias correction are expected to cancel in the scene-by-scene subtraction, it is still desirable to have accurate retrievals. A larger dataset will allow for a better clear sky radiance bias correction, which is the likely cause of large biases between simulated heights and lidar heights from CALIOP.

The MODIS collection 6 CTH retrieval algorithm uses gridded bias corrections averaged over several days, while this study uses just a single value averaged over all latitudes for each day. An error in surface emissivity over desert or snow will not affect the entire day's radiances, so a regionally based bias correction should decrease differences from lidar retrievals.

The completion of the simulator algorithm will allow many more inter-comparison studies to be performed. To test the sensitivity of CO₂ slicing to a violation of the assumption of identical cloud emissivity for the two channels, small and incremental bias factors will be applied to the right hand side of Eqn. 3. Zhang and Menzel (2002) performed a similar study, but the simulator algorithm allows for simulation of any instrument, not just MODIS, allowing for general statements to be made.

References

- Anderson, GP., Clough, SA., Kneizys, FX., Chetwynd, JH., & Shettle, EP. Air Force Geophysics Laboratory, Optical Physics Division. (1986). *AFGL atmospheric constituent profiles (0-120km)* (AFGL-TR-86-0110). Hanscom AFB, MA: Environmental Research Papers.
- Aumann, HH., Chahine, MT., Gautier, C., Goldberg, MD., Kalnay, E., McMillin, LM., Revercomb, H., Rosenkranz, PW., Smitch, WL., Staelin, DH., Strow, LL., & Susskind, J. (2003). AIRS/AMSU/HSB on the Aqua mission: design, science objectives, data products, and processing systems. *IEEE Transactions on Geoscience and Remote Sensing*, 41(2), 253-264.
- Barnes, WL., Xiong, X., & Salomonson, VV. (2003). Status of Terra MODIS and Aqua MODIS. *Advances in Space Research*, 32(11), 2099-2106.
- Baum, BA., & Wielicki, BA. (1994). Cirrus cloud retrieval using infrared sounding data - multilevel cloud errors. *Journal of Applied Meteorology*, 33(1), 107-117.
- Clough, SA., Kneizys, FX., Rothman, LS., & Gallery, WO. Atmospheric spectral transmittance and radiance: FASCODE1B, *Proc. Soc. Photo. Opt. Instrum. Eng.*, 277, 152-166, 1981.
- Clough, S., Iacono, M., & Moncet, JL. (1992), Line-by-Line Calculations of Atmospheric Fluxes and Cooling Rates: Application to Water Vapor, *J. Geophys. Res.*, 97(D14), 15761-15785.
- Hannon, S., L. L. Strow, and W. W. McMillan. (1996): Atmospheric infrared fast transmittance models: A comparison of two approaches. Proc. Conf. on Optical Spectroscopic Techniques and Instrumentation for Atmospheric and Space Research II, Denver, CO, SPIE, 94-105.
- Holz, RE., Ackerman, S., Antonelli, P., Nagle, F., Knuteson, RO., Hlavka, KL., & Hart, WD. (2006). An improvement to the high-spectral-resolution CO₂-slicing cloud-top altitude retrieval. *Journal of the Atmospheric and Oceanic Technology*, 23(5), 653-670.
- Jacobowitz, H. (1970). *Emission, scattering and absorption of radiation in cirrus cloud layers*. Massachusetts Institute of Technology. Dept. of Meteorology.
- Jacobowitz, H., Stowe, LL., Ohring, G., Heidinger, A., Knapp, K. & Nalli, NR. (2003). The advanced very high resolution radiometer pathfinder atmosphere (patmos) climate dataset - a resource for climate research. *Bulletin of the American Meteorological Society*, 84(6), 785-793.

Kanamitsu, M., Alpert, J.C., Cmpana, K.A., Caplan, P.M., Deaven, D.G., Iredell, M., Katz, B., Pan, H.L., Sela, J., & White, G.H. (1991). Recent changes implemented into the global forecast system at NMC. *Weather and Forecasting*, 6(3), 425-435.

Key, J.R., & Schweiger, A.J. (1998). Tools for atmospheric radiative transfer: streamer and fluxnet. *Computers and Geosciences*, 24(5), 443-451.

Menzel, W.P., Wylie, D.P., & Strabala, K.I. (1992). Seasonal and diurnal changes in cirrus clouds as seen in four years of observations with the VAS. *Journal of Applied Meteorology*, 31(4), 370-385.

Menzel, W.P., Frey, R.A., Zhang, H., Wylie, D.P., Moeller, C.C., Holz, R.E., Maddux, B., Baum, B.A., Strabala K.I., & Gumley, L.E. (2008). MODIS global cloud-top pressure and amount estimation: algorithm description and results. *Journal of Applied Meteorology and Climatology*, 47(4), 1175-1198.

Nagle, F.W., & Holz, R.E. (2009). Computationally efficient methods of collocating satellite, aircraft, and ground observations. *Journal of the Atmospheric and Oceanic Technology*, 26(8), 1585-1595.

"NOAA TOVS/ATOVS" *Comprehensive Large Array-Data Stewardship System (CLASS)*. N.p., n.d. Web. 4 Aug 2011.
<http://www.nsof.class.noaa.gov/release/data_available/tovs_atovs/index.htm#hirs2>.

Petty, G.W. (2006). *A first course in atmospheric radiation*. Madison, WI: Sundog Publishing.

Rossow, W.B., & Schiffer, R.A. (1999). Advances in understanding clouds from ISCCP. *Bulletin of the American Meteorological Society*, 80(11), 2261-2287.

Sassen, K., Z. Wang, & D. Liu (2008), Global distribution of cirrus clouds from CloudSat/Cloud-Aerosol Lidar and Infrared Pathfinder Satellite Observations (CALIPSO) measurements, *J. Geophys. Res.*, 113, D00A12, doi:10.1029/2008JD009972.

Senior, C.A., & Mitchell, J.F.B. (1993). Carbon-dioxide and climate - the impact of cloud parameterization. *Journal of Climate*, 6(3), 393-418.

Smith, W.L., Woolf, H.M., Abel, P.G., Hayden, C.M., & Chalfant, Mark. National Oceanic and Atmospheric Administration, (1974). *Nimbus-5 sounder data processing system* (19750007254)

Spinhirne, J.D., & Hart, W.D. (1990). Cirrus structure and radiative parameters from airborne lidar and spectral radiometer observations - the 28 October 1986 fire study. *Monthly Weather Review*, 118(11), 2329-2343.

Stephens, GL., & Webster, PJ. (1981). Clouds and climate - sensitivity of simple systems. *Journal of the Atmospheric Sciences*, 38(2), 235-247.

Stephens, GL. (2005). Cloud feedbacks in the climate system: a critical review. *Journal of Climate*, 18(2), 237-273.

Strow, LL., Hannon, SE., Weiler, M., Overoye, K., Gaiser, SL., & Aumann, HH. (2003). Prelaunch spectral calibration of the Atmospheric Infrared Sounder (AIRS). *IEEE Transactions on Geoscience and Remote Sensing*, 41(2), 274-286.

Tobin, DC., Revercomb, HE., Moeller, CC., & Pagano, TS. (2006). Use of Atmospheric Infrared Sounder high-spectral resolution spectra to assess the calibration of moderate resolution imaging spectroradiometer on EOS Aqua. *Journal of Geophysical Research - Atmospheres*, 111(D9).

Vaughan, M., Young, S., Winker, D., Powell, K., Omar, A., Liu, Z., Hu, Y., & Hostetler, C. (2004). Fully automated analysis of space-based lidar data: an overview of the CALIPSO retrieval algorithms and data products. *Proceedings of the Laser radar techniques for atmospheric sensing* (pp. 16-30). Bellingham, WA: SPIE. 10.1117/12.572024.

Wylie, DP., & Menzel, WP. (1999). Eight years of high cloud statistics using HIRS. *Journal of Climate*, 12(1), 170-184.

Wylie, D., Jackson, DL., Menzel, WP., & Bates, JJ. (2005). Trends in global cloud cover in two decades of HIRS observations. *Journal of Climate*, 18(15), 3021-3031.

Zhang, H., & Menzel, WP. (2002). Improvement in thin cirrus retrievals using an emissivity-adjusted CO₂ slicing algorithm. *Journal of Geophysical Research-Atmospheres*, 107(D17).

Zhang, Hong, Richard Frey, and Paul Menzel. "Sensitivity Study of the MODIS Cloud Top Property Algorithm to CO₂ Spectral Response Functions." *Proceedings of the Fourteenth International TOVS Study Conference*. Roger Saunders and Thomas Ahtor: Beijing, China, 2005. 130-137. PDF.